Progress of Theoretical Physics, Vol. 119, No. 2, February 2008

Some Properties of the Resonant State in Quantum Mechanics and Its Computation

Naomichi HATANO,[1,*] Keita SASADA,[2] Hiroaki NAKAMURA[3] and Tomio PETROSKY[4]

[1]*Institute of Industrial Science, University of Tokyo, Tokyo 153-8505, Japan*
[2]*Department of Physics, University of Tokyo, Tokyo 153-8505, Japan*
[3]*Department of Simulation Science, National Institute for Fusion Science, Gifu 509-5292, Japan*
[4]*Center for Complex Quantum Systems, University of Texas at Austin, 1 University Station, C1609, Austin, TX 78712, USA*

(Received August 21, 2007)

The resonant state of open quantum systems is studied from the viewpoint of the eigenfunction with an outgoing momentum flux. We show that the number of particles is conserved for a resonant state if we use an expanding volume of integration in order to take account of the outgoing momentum flux; the number of particles in a fixed volume of integration would decay exponentially. Moreover, we introduce new numerical methods of treating the resonant state with the use of an effective potential. We first present a numerical method for finding a resonance pole in the complex energy plane. This method seeks an energy eigenvalue iteratively. We found that it leads to super-convergence, i.e., convergence whose rate is exponential with respect to the iteration step. Also, it is independent of the commonly used complex scaling. We also present a numerical trick for computing the time evolution of the resonant state in a limited spatial area. Because the wave function of the resonant state is diverging away from the scattering potential, it is difficult to follow its time evolution numerically in a finite area using previous methods.

§1. Introduction

Resonance phenomena have been studied extensively for a long time.[1)–20)] They appear in almost every field of physics, from classical mechanics to quantum mechanics. In spite of this fact, however, many fundamental aspects of resonance phenomena, e.g., applications to many-body quantum systems,[21)] remain to be investigated. Particularly, in condensed matter and statistical physics, many textbooks introduce the resonant state only as a pole of the scattering matrix and do not elaborate further. There are, in fact, two ways of defining and finding a resonant state in quantum mechanics.[22),23)] Introducing it as a pole of the scattering matrix[3),6),18)] is sometimes called the "indirect method". In the "direct method",[22),23)] contrastingly, we define and compute the resonant state as an explicit solution of the Schrödinger equation with a complex eigenvalue and a diverging eigenfunction.[2),14)–16)] The latter method may be advantageous for generalizing the concept to many-body problems and is increasingly used in nuclear physics. However, the direct method has been largely ignored in the field of condensed matter physics. Given this situation, it is

*) E-mail: hatano@iis.u-tokyo.ac.jp

noteworthy that Nishino and one of the present authors (N.H.)[21] recently analytically obtained an explicit form of the many-body scattering eigenfunction for an open quantum-dot system with a Coulomb interaction.

Despite their long history, resonance phenomena have recently become of increasing importance, especially in the quantum mechanics of mesoscopic devices. When we use nano-devices, we inevitably must attach leads to them. Hence such devices are always open quantum systems and possess resonant states: An electron enters a device through a lead, is trapped in the confining potential of the device for a finite time, and then may exit through another lead. Such resonant conduction of mesoscopic systems has been extensively studied experimentally; for example, the Fano resonance[24)–27)] has attracted much attention. Because the Coulomb interaction is fundamental in many experiments, we believe that the direct method of defining and obtaining resonant states will be increasingly important in condensed matter physics.

In the present paper, we study resonant states of open quantum systems mainly in the framework of the direct method. The paper consists of two parts. In the first part, from §2 to §4, we study the physical significance of the imaginary part of the resonant eigenvalue in a somewhat pedagogical manner, with condensed matter and statistical physicists as the target audience. When we have previously presented our results in various contexts, we have received many questions regarding well-established knowledge concerning resonant states (particularly in the framework of the direct method) from condensed matter and statistical physicists, and hence we find it necessary to review here fundamental properties of resonant states to make the paper self-contained.

In addition to this well-established knowledge, we include two new points in our discussion. First, we show that

> the imaginary part of the energy expectation is proportional to the outgoing momentum flux for *arbitrary* wave functions.

Such a relation has appeared in the literature, but for *individual* resonant states,[28)–30)] in which case the imaginary part of the energy expectation reduces to the lifetime, or the half-width, of the resonance and the momentum flux reduces to the real part of the wave number of the eigenstate.

Second, we show that

> the number of particles in a resonant state is *conserved* when we count the number in an expanding volume.

The resonant state represents a decaying state, and its particle number decreases exponentially *if we count the number in a fixed volume*. Because the decay rate is related to the outgoing momentum flux, as stated above, we can keep track of leaking particles by employing an constantly expanding volume of integration. As far as we know, this fact has not previously been pointed out in the literature, despite its simplicity.

In the second part of the paper, §§5 and 6, we introduce new numerical methods of treating the resonant state that uses an effective potential.[31)–42)] A logical conclusion of the arguments given in §§2 and 3 is that the eigenfunction of the resonant state is diverging away from the scattering potential. For this reason, treating resonant states numerically in the framework of the direct method (that is, as an explicit solution of the Schrödinger equation) could involve difficulties. The naive approximation consisting of simply truncating the infinite space would necessarily fail, except, perhaps, in the case of resonant states with long lifetimes; a resonant state never appears in a closed system, and a diverging eigenfunction cannot be represented precisely in a finite space, although it is possible to approximate a resonant eigenfunction with slow divergence by a bound state function. (See Ref. 43) for an explicit example.) A conventional method within the framework of the direct method is to suppress the divergence by employing complex scaling, or complex rotation.[14)–16),30),44)–53)] (See, e.g., Ref. 18) for studies in the framework of the indirect method.)

Here we use an effective potential consisting of an energy dependent boundary conditions, in order to truncate the infinite space. We can thereby find resonance poles in the complex energy plane, working in a finite space. The present method seeks the energy eigenvalue iteratively. We numerically demonstrate for a simple model that we can indeed find a complex eigenvalue of the resonance pole. We found that our method is rapidly converging, as in the KAM theory[54),55)] of nonlinear dynamics and the Newton method for determining the solutions of nonlinear equations; specifically, the rate of convergence is exponential with respect to the iteration step. We can also compute the time evolution of the resonant state in a finite space. We numerically demonstrate for the Friedrichs model that we can determine the dynamics of the central part of the diverging resonant eigenfunction. Numerical calculations for a ladder lattice in which we determine quasi-stable resonant states with very long lifetimes are reported elsewhere.[43)]

§2. The imaginary part of the energy expectation

In the present section, we show that the imaginary part of the energy expectation is proportional to the flux out of a volume as well as the lifetime of the resonant state. Thus, the energy is generally complex in an open quantum system. Such a relation has previously been obtained only for individual resonant states.

Hereafter, we consider the one-dimensional case to simplify the explanation. (See Appendix A.1 for the corresponding expressions in the three-dimensional case.) Consider the one-dimensional one-body Hamiltonian,

$$\hat{\mathcal{H}} = \hat{\mathcal{K}} + \hat{\mathcal{V}}, \tag{2·1}$$

where

$$\hat{\mathcal{K}} \equiv \frac{\hat{p}^2}{2m} = -\frac{\hbar^2}{2m}\frac{d^2}{dx^2} \quad \text{and} \quad \hat{\mathcal{V}} \equiv V(x). \tag{2·2}$$

We assume that the potential operator $\hat{\mathcal{V}}$ has finite support:

$$\Omega_{\rm pot} \equiv \{x \mid -l \le x \le l\}; \tag{2·3}$$

that is, we assume that the potential function is reasonably localized around the origin. We also assume that the potential operator is Hermitian and, thus, that the potential function is real:

$$V(x)^* \equiv V(x). \tag{2·4}$$

We see below that the kinetic energy is not necessarily a Hermitian operator.

2.1. *The imaginary part and the momentum flux*

Let us next determine whether the Hamiltonian (2·1) is a Hermitian operator. We can do this by finding whether the expectation value of the Hamiltonian operator is real for an arbitrary wave function $\psi(x)$. We define the Hamiltonian expectation value as follows:

$$\langle\psi|\hat{\mathcal{H}}|\psi\rangle_\Omega \equiv \int_{-L}^{L} \psi(x)^* \hat{\mathcal{H}}\psi(x)dx. \tag{2·5}$$

Note here that the volume of the integration is limited to a segment

$$\Omega \equiv \{x \mid -L \le x \le L\} \tag{2·6}$$

that includes the support of the potential operator $\hat{\mathcal{V}}$; that is, we assume $\Omega \supset \Omega_{\rm pot}$, or $L > l$. The reason for limiting the integration volume becomes clear below. The usual definition of the expectation value is recovered in the infinite-segment limit after normalization:

$$\langle\psi|\hat{\mathcal{H}}|\psi\rangle \equiv \lim_{|\Omega|\to\infty} \frac{\langle\psi|\hat{\mathcal{H}}|\psi\rangle_\Omega}{\langle\psi|\psi\rangle_\Omega}. \tag{2·7}$$

We now compute the imaginary part of the expectation value,

$$2i\,{\rm Im}\langle\psi|\hat{\mathcal{H}}|\psi\rangle_\Omega = \langle\psi|\hat{\mathcal{H}}|\psi\rangle_\Omega - \left(\langle\psi|\hat{\mathcal{H}}|\psi\rangle_\Omega\right)^*, \tag{2·8}$$

and determine the cases in which it is non-zero. Owing to the assumption that the potential is a real, localized function, the expectation value of the potential term must be real. Therefore, only the kinetic term contributes to Eq. (2·8). The expectation value of the kinetic term is transformed using integration by parts as

$$\begin{aligned}\langle\psi|\hat{\mathcal{K}}|\psi\rangle_\Omega &= -\frac{\hbar^2}{2m}\int_{-L}^{L} \psi(x)^*\psi''(x)dx \\ &= \frac{\hbar^2}{2m}\int_{-L}^{L} \psi'(x)^*\psi'(x)dx - \frac{\hbar^2}{2m}\left[\psi(x)^*\psi'(x)\right]_{x=-L}^{L}.\end{aligned} \tag{2·9}$$

The first term on the right-hand side of Eq. (2·9) is real. The second term, however, can be complex, which results in a non-zero imaginary part of the Hamiltonian expectation value.

Subtracting out the complex conjugate from Eq. (2·9), we have

$$\begin{aligned} 2i\,\mathrm{Im}\langle\psi|\hat{\mathcal{H}}|\psi\rangle_{\Omega} &= -\frac{\hbar^2}{2m}\left[\psi(x)^*\psi'(x) - \psi(x)\psi'(x)^*\right]_{x=-L}^{L} \\ &= -\frac{i\hbar}{m}\,\mathrm{Re}\left(\psi(x)^*\hat{p}\psi(x)\big|_{x=L} - \psi(x)^*\hat{p}\psi(x)\big|_{x=-L}\right), \end{aligned} \tag{2·10}$$

where $\hat{p}$ is the momentum operator. For the purpose of generalizing the above expression to higher-dimensional cases, we write the last line as

$$\langle\psi|\hat{p}_{\mathrm{n}}|\psi\rangle_{\partial\Omega} \equiv \psi(x)^*\hat{p}\psi(x)\big|_{x=L} - \psi(x)^*\hat{p}\psi(x)\big|_{x=-L}, \tag{2·11}$$

where $\hat{p}_{\mathrm{n}}$ is the component of the momentum normal to the surface $\partial\Omega$. This represents the momentum flux out of the segment Ω. Thus we arrive at

$$\mathrm{Im}\langle\psi|\hat{\mathcal{H}}|\psi\rangle_{\Omega} = -\frac{\hbar}{2m}\,\mathrm{Re}\langle\psi|\hat{p}_{\mathrm{n}}|\psi\rangle_{\partial\Omega}. \tag{2·12}$$

This is a very useful formula in the analysis of resonant states.

We have shown this general result for arbitrary wave functions. This relation, however, has already been derived for individual resonant states; see, e.g., Eq. (2.13) of Ref. 28), Eq. (24) of Ref. 29) and Eq. (3.19) of Ref. 30). For each resonant state $\psi_{\mathrm{res},n}$, the energy expectation value reduces to the complex eigenvalue

$$\lim_{|\Omega|\to\infty} \frac{\langle\psi|\hat{\mathcal{H}}|\psi\rangle_{\Omega}}{\langle\psi|\psi\rangle_{\Omega}} = \varepsilon_n - i\frac{\Gamma_n}{2}, \tag{2·13}$$

as reviewed in §4.1, while the momentum flux reduces to

$$\mathrm{Re}\langle\psi|\hat{p}_{\mathrm{n}}|\psi\rangle_{\partial\Omega}. = \hbar k_n, \tag{2·14}$$

again, as reviewed in §4.1. Taking account of the normalization factor $1/\sqrt{2\kappa_n}$ of the resonant wave function, we see that the relation (2·12) reduces to

$$\frac{\Gamma}{4\kappa_n} = \frac{\hbar^2}{2m}k_n, \tag{2·15}$$

which has been obtained previously[28)–30)] and is derived in a different context in §3.2.

The formula (2·12) asserts that the imaginary part of the energy expectation value represents the outgoing momentum flux. This leads to the following observation:

> The Hamiltonian (the kinetic term, in particular) is a Hermitian operator if the system is closed but is generally a non-Hermitian operator if it is open.

The Hamiltonian of an open system is Hermitian only when the incoming flux balances the outgoing flux. Conversely, if we *assume* that the Hamiltonian of an open

system is Hermitian from the beginning, the flux must be conserved. Indeed, it is seen in the textbook example of tunneling phenomena that the sum of the reflection flux and the transmission flux is equal to the incident flux. In fact, this physically reasonable phenomenon of flux conservation is, from an algebraic point of view, a consequence of the assumption that the energy variable is real.

2.2. *The imaginary part and the lifetime*

Now we present a familiar relation between the imaginary part of an eigenvalue and the decay rate of the resonant state (see, e.g., Ref. 56)). Here we consider the time-dependent Schrödinger equation

$$i\hbar\frac{\partial}{\partial t}\Psi(x,t) = \hat{\mathcal{H}}\Psi(x,t). \tag{2·16}$$

We compute the time dependence of the particle number in the segment Ω, given by

$$N_\Omega(t) \equiv \langle\Psi|\Psi\rangle_\Omega. \tag{2·17}$$

Its time derivative transforms as

$$\begin{aligned}\frac{d}{dt}N_\Omega(t) &= \int_{-L}^{L}\left(\Psi(x,t)^*\frac{\partial\Psi(x,t)}{\partial t} + \frac{\partial\Psi(x,t)^*}{\partial t}\Psi(x,t)\right)dx \\ &= -\frac{i}{\hbar}\int_{-L}^{L}\left[\Psi(x,t)^*\hat{\mathcal{H}}\Psi(x,t) - \Psi(x,t)\left(\hat{\mathcal{H}}\Psi(x,t)\right)^*\right]dx \\ &= \frac{2}{\hbar}\,\mathrm{Im}\langle\Psi|\hat{\mathcal{H}}|\Psi\rangle_\Omega. \end{aligned}\tag{2·18}$$

Note that the last line of Eq. (2·18) is related to the momentum flux in Eq. (2·12) as

$$\frac{d}{dt}N_\Omega(t) = \frac{2}{\hbar}\,\mathrm{Im}\langle\Psi|\hat{\mathcal{H}}|\Psi\rangle_\Omega = -\frac{1}{m}\,\mathrm{Re}\langle\Psi|\hat{p}_\mathrm{n}|\Psi\rangle_{\partial\Omega}. \tag{2·19}$$

We thus conclude that the imaginary part of the Hamiltonian expectation value is related to two quantities, the outgoing momentum flux and the decay rate of the particle number in the system. This is a very natural conclusion, as the decrease of the particle number is due only to leaking from the system (Fig. 1).

Equation (2·19) also indicates that treating a complex energy eigenvalue is closely related to treating the complex momentum of the corresponding eigenstate.

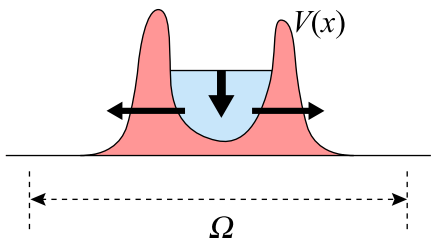

Fig. 1. The decrease of the particle number is equal to leaking from the system.

In fact, we have found that in some cases it is more convenient to solve the problem in the complex momentum plane than in the complex energy plane, which we demonstrate below.

§3. Resonant state as a solution of the stationary Schrödinger equation

The facts established in the previous section indicate that an open quantum system can possess an eigenstate with a complex eigenvalue. In the present paper, we generally refer to such a state as a "resonant state".

As mentioned in the Introduction, there are mainly two ways of defining the resonant state.[23] In the present paper, we focus on the direct method, in which we define the resonant state as an explicit solution of the Schrödinger equation. In the present section, particularly in §§3.1 and 3.2, we show that a resonant state is an eigenfunction of the Hamiltonian of an open quantum system under the boundary condition that we have only outgoing waves. By contrast, the indirect method, which is employed in many textbooks,[17),18)] defines a resonant state as a pole of the scattering matrix or a zero of the Jost function. We show in §3.3 that the two definitions are indeed equivalent. It is notable, however, that the direct method naturally gives the parity of the resonant state, as we demonstrate in §3.2.

The assertions made in this section have all been presented previously, except for the comment on a resonance peak of the transmission probability presented in §§3.2 and 3.3. Readers familiar with resonant states may skip to §3.2. The (perhaps) new contribution of the present section is the observation that a resonance peak of the transmission probability does not necessarily correspond to a resonant eigenstate. We show in an illustrative example, specifically in Figs. 4(d) and (e), that the lowest peak of the transmission probability, or the conductance, cannot be regarded as a resonance peak because the corresponding resonant eigenstate is missing.

3.1. *Defining the resonant state as an eigenfunction*

We now show that we can obtain eigenstates with complex eigenvalues by solving the stationary Schrödinger equation under a certain boundary condition. Specifically, the boundary condition is that there exist outgoing waves only, no incoming waves. In this case, the momentum is obviously not conserved, and hence the eigenvalue is complex, as indicated by Eq. (2·12). In most textbooks, by contrast, a quantum resonant state is defined as a singularity of the S matrix. We argue that this definition (sometimes called the indirect method) is equivalent to the present definition (sometimes called the direct method).

We again study the one-dimensional case. As in the previous section, we have a potential $V(x)$ in the finite region $\Omega_{\rm pot}$ defined in Eq. (2·3). Outside this region, we have only the kinetic term in the Hamiltonian, i.e.

$$V(x) = 0 \quad \text{for} \quad x \notin \Omega_{\rm pot}, \tag{3·1}$$

and hence any eigenfunction is composed of plane waves $\exp(\pm iKx)$ with

$$K = \frac{\sqrt{2mE}}{\hbar}. \tag{3·2}$$

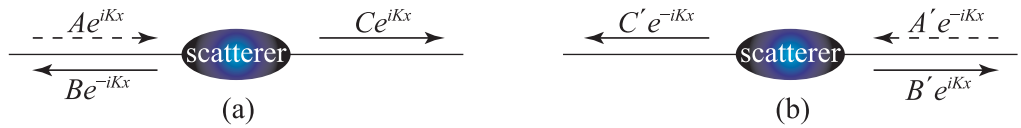

Fig. 2. The S matrix of a scattering potential is defined in terms of two scattering solutions as in (a) and (b). Singularities of the S matrix appear when the incident waves are missing.

The argument given in the previous section shows that a momentum flux going out of the central area [Ω defined in Eq. (2·6)] may yield a state with a complex eigenvalue. This motivates us to seek an eigenstate with boundary conditions such that there exist outgoing waves only:

$$\psi_{\rm res}(x) = \begin{cases} Be^{-iKx} & \text{for } x < -L, \\ Ce^{iKx} & \text{for } x > L. \end{cases} \tag{3·3}$$

This set of boundary conditions is often called the Siegert condition[2),17)] and has been used occasionally in the literature. If there exists an eigenfunction satisfying Eq. (3·3) with $\mathrm{Re}\, K > 0$, it obviously has a finite momentum flux going out of the central area, and hence its energy eigenvalue E must be complex, because of formula (2·12).

In the present paper, we define the resonant state in the following way:

> A resonant state is a solution of the Schrödinger equation (an eigenfunction of the Hamiltonian) under boundary conditions such that only outgoing waves exist outside the segment Ω.

We show below that this definition (the direct method) is equivalent to seeking poles of the S matrix of the potential (the indirect method).

In order to define the S matrix, we consider an eigenfunction satisfying the following boundary conditions (Fig. 2) instead of Eq. (3·3):

$$\psi(x) = \begin{cases} Ae^{iKx} + Be^{-iKx} & \text{for } x < -L, \\ Ce^{iKx} & \text{for } x > L. \end{cases} \tag{3·4}$$

In order for Eq. (3·4) to be a solution of the stationary Schrödinger equation $\hat{\mathcal{H}}\psi(x) = E\psi(x)$, the coefficients A, B and C must depend on E. The momentum flux out of the central area Ω can vanish for this set of boundary conditions whenever the outgoing flux is balanced by the incoming flux: $|A(E)|^2 = |B(E)|^2 + |C(E)|^2$. Thus, an eigenstate satisfying Eq. (3·4) has a real energy eigenvalue.

The S matrix in one dimension is defined as follows. The reflection amplitude from the left back to the left is given by

$$r_{\rm LL}(E) \equiv \frac{B(E)}{A(E)}, \tag{3·5}$$

while the transmission amplitude from the left to the right is given by

$$t_{\rm RL}(E) \equiv \frac{C(E)}{A(E)}. \tag{3·6}$$

Similarly, we can consider an eigenfunction satisfying

$$\psi(x) = \begin{cases} C'e^{-iKx} & \text{for } x < -L, \\ A'e^{-iKx} + B'e^{iKx} & \text{for } x > L, \end{cases} \tag{3·7}$$

and have the reflection amplitude from the right back to the right and the transmission amplitude from the right to the left as

$$r_{\mathrm{RR}}(E) \equiv \frac{B'(E)}{A'(E)} \quad \text{and} \quad t_{\mathrm{LR}}(E) \equiv \frac{C'(E)}{A'(E)}. \tag{3·8}$$

The S matrix in this case is then defined as

$$S \equiv \begin{pmatrix} r_{\mathrm{LL}} & t_{\mathrm{LR}} \\ t_{\mathrm{RL}} & r_{\mathrm{RR}} \end{pmatrix}, \tag{3·9}$$

which relates the incoming waves from the left and the right to the outgoing waves to the left and the right.

The indirect method defines the resonant state as a singularity of the S matrix analytically continued onto the complex E plane. The elements of the S matrix in fact diverge whenever

$$A(E) = 0 \quad \text{or} \quad A'(E) = 0. \tag{3·10}$$

We note that the set of boundary conditions (3·4) reduces to Eq. (3·3) when $A(E) = 0$. Instead of solving the Schrödinger equation under the boundary conditions (3·4) *and then* seeking the zeros of $A(E)$, Eq. (3·3) implies that we solve the Schrödinger equation with $A(E) = 0$ from the very beginning. Except for this difference, the direct and indirect methods of defining the resonant state are indeed equivalent.

It might seem that the outgoing waves in Eq. (3·3) spring out of nowhere, but this is, of course, not true. The particles acting as the source of the outgoing waves exist in the trapping potential from the beginning. The particle probability leaks from the potential at a rate proportional to the particle probability itself; note that the right-hand side of Eq. (2·19) has the factor $\exp(-t \operatorname{Im} E/\hbar)$. Hence, the particle probability in the trapping potential decreases, and so does the leaking probability. The particle probability decreases exponentially forever, as the leak decreases forever (see §4 for more details). Because here we define a resonant state as a stationary state, we can only describe a resonance as above. In this picture, we do not employ the dynamic description of a resonance, according to which a particle enters the scattering potential from outside, is trapped by the potential for a while, and then escapes.

3.2. *Illustrative example*

Here we confirm the above arguments, solving a simple example in one dimension. We also present the observation that a resonance peak of the transmission probability does not necessarily correspond to a resonant eigenstate.

Let us consider a potential consisting of two delta functions:

$$V(x) = V_0 \left(\delta\left(x + l\right) + \delta\left(x - l\right)\right). \tag{3·11}$$

In order to obtain the resonant state for this potential, we assume the form

$$\psi_{\rm res}(x) = \begin{cases} Be^{-iKx} & \text{for } x < -l, \\ Fe^{iKx} + Ge^{-iKx} & \text{for } -l < x < l, \\ Ce^{iKx} & \text{for } x > l. \end{cases} \tag{3·12}$$

Note that only outgoing waves exist outside the potential. The connection conditions at $x = \pm l$ are given by

$$\psi_{\rm res}(\pm l + 0) - \psi_{\rm res}(\pm l - 0) = 0, \tag{3·13}$$

$$\psi'_{\rm res}(\pm l + 0) - \psi'_{\rm res}(\pm l - 0) = a^{-1}\psi_{\rm res}(\pm l), \tag{3·14}$$

where the length scale a is defined by

$$a \equiv \frac{\hbar^2}{2mV_0}. \tag{3·15}$$

The solution (3·12) has four undetermined constants (the energy eigenvalue E and the three ratios of the coefficients B, C, F and G), while we have four connection conditions, Eqs. (3·13)–(3·14). Hence we can fix the energy eigenvalues to discrete values.

We can simplify the solution further. Because the potential (3·11) is an even function, its solutions can be classified according to their parities. The even and odd solutions are given by

$$B = \pm C \quad \text{and} \quad G = \pm F, \tag{3·16}$$

respectively. Solutions of a definite parity have two undetermined constants (the energy eigenvalue E and the ratio of C and F), while there are two independent connection conditions at $x = +l$. Eliminating the coefficients C and F, we arrive at

$$1 - 2iKa = \mp e^{2iKl}, \tag{3·17}$$

where the upper sign corresponds to the even solutions and the lower sign to the odd ones. This equation determines discrete wave numbers K_n, and hence it determines discrete energy eigenvalues $E_n = \hbar^2 K_n^2/2m$ in the complex energy plane.

For numerical calculations, we set

$$K_n \equiv k_n - i\kappa_n, \tag{3·18}$$

where $k_n > 0$. Equation (3·17) can then be rewritten as

$$\eta_n = \frac{l}{2a} + \frac{\xi_n}{\tan 2\xi_n}, \tag{3·19}$$

$$\xi_n = \pm\frac{l}{2a}\sqrt{e^{4\eta_n} - \left(1 - \frac{2a}{l}\eta_n\right)^2}, \tag{3·20}$$

where $\xi_n \equiv k_n l$ and $\eta_n \equiv \kappa_n l$. In Fig. 3, we plot the functions (3·19) and (3·20) in the region $\xi = kl > 0$ for the cases $a/l = 0.1$, 1, 4 and 10. The intersection points

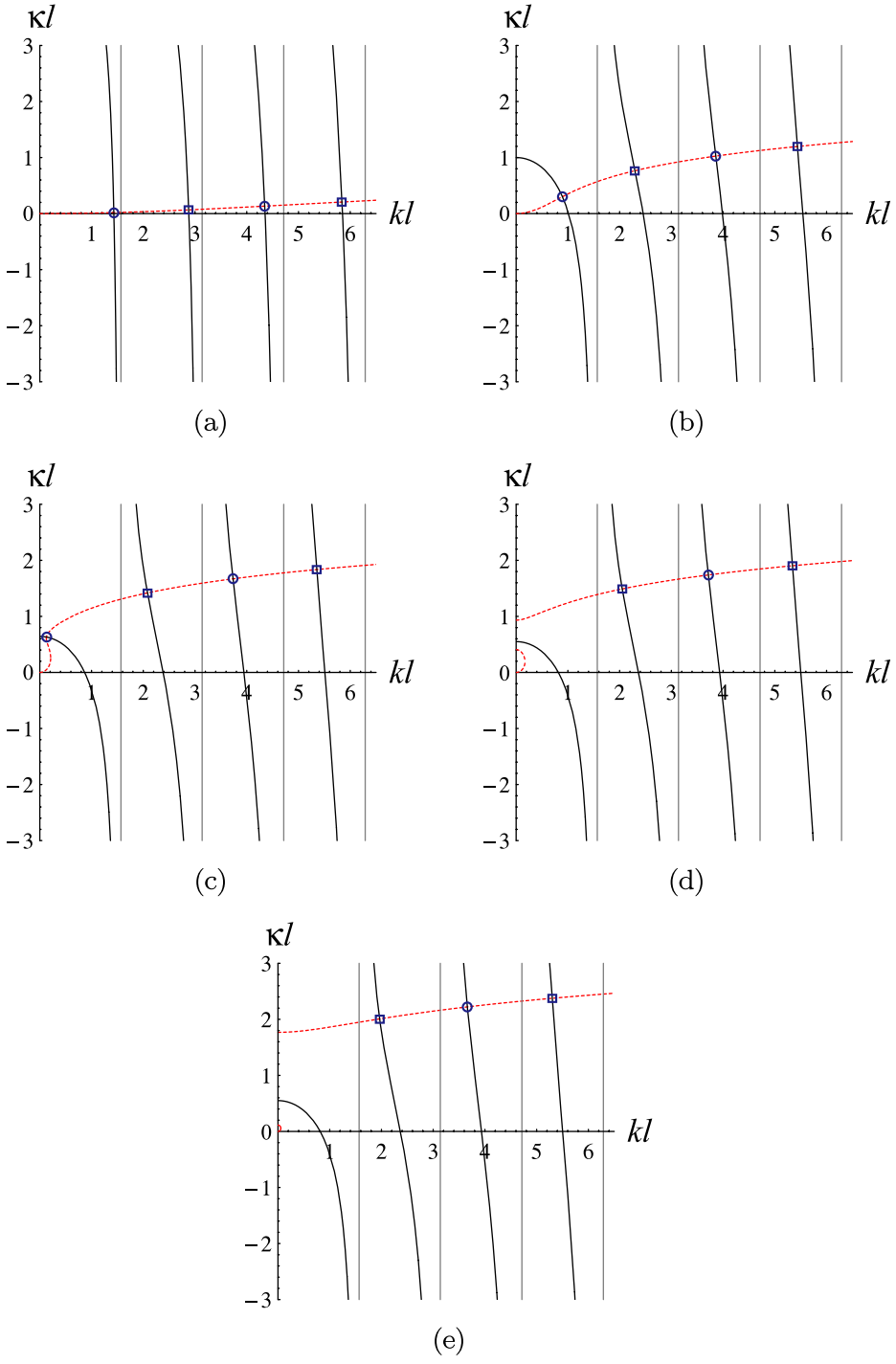

Fig. 3. Plots of Eq. (3·19) (solid curves) and Eq. (3·20) (broken curves) in the cases (a) $a/l = 0.1$, (b) $a/l = 1$, (c) $a/l = 3.5$, (d) $a/l = 4$ and (e) $a/l = 10$. The vertical thin gray lines indicate $kl = n\pi$, which are the bound states for $V_0 \to \infty$, or $a = 0$. The circles represent even solutions and the squares represent odd solutions. Note that the first even solution disappears in (d) and (e).

represent the solutions; the circles denote solutions with even parity and the squares denote solutions with odd parity. There are also solutions in the region $\xi = kl < 0$ with a negative real part $-\xi_n$ and the same imaginary part η_n; Equations (3·19) and (3·20) are symmetric with respect to the η axis if we take into account the sign of the right-hand side of Eq. (3·20).

The lowest even solution disappears for $a/l > 3.59112\cdots$. The curve described by Eq. (3·20) splits into two branches for $a/l > 3.59112\cdots$, one circling near the origin, and the other continuing to infinity. In the cases depicted in Figs. 3 (d) and (e), there is a small branch near the origin, which does not intersect with the curve described by Eq. (3·19). Nevertheless, the remnant of the resonance peak corresponding to this missing pole exists in the transmission probability; see the last paragraph of §3.3 below. We have never seen this phenomenon reported previously.

Note here that all solutions (the intersection points in Fig. 3) satisfy

$$\kappa_n = -\operatorname{Im} K_n > 0. \tag{3·21}$$

In Table I, we list numerical estimates (obtained using Mathematica) for the solutions K_n and the resulting energy eigenvalues,

$$E_n = \frac{\hbar^2 K_n^2}{2m} \equiv \varepsilon_n - i\frac{\Gamma_n}{2}. \tag{3·22}$$

The solutions with $k_n \equiv \operatorname{Re} K_n > 0$ have outgoing waves only, whereas the solutions with $k_n < 0$ (not shown in Fig. 3) have incoming waves only. We note here

Table I. Numerical estimates of the complex wave numbers and complex eigenvalues of the first few resonant states for the double delta potential (3·11). The solutions with $\operatorname{Re} K_n > 0$ and $\operatorname{Im} E_n < 0$ are plotted in Fig. 3. Note that the first even solution disappears in the cases $a/l = 4$ and $a/l = 10$.

a/l	state (parity)	$K_n = k_n - i\kappa_n$ $[1/l]$	$E_n = \varepsilon_n - i\Gamma_n/2$ $[\hbar^2/ml^2]$
0.1	1st (even)	$\pm 1.430948 - i0.018013$	$1.023644 \mp i0.025776$
	2nd (odd)	$\pm 2.877577 - i0.066510$	$4.138014 \mp i0.191389$
	3rd (even)	$\pm 4.347821 - i0.133182$	$9.442907 \mp i0.579054$
	4th (odd)	$\pm 5.841379 - i0.206480$	$17.039540 \mp i1.206128$
1	1st (even)	$\pm 0.894094 - i0.302510$	$0.353945 \mp i0.270472$
	2nd (odd)	$\pm 2.298579 - i0.766046$	$2.348319 \mp i1.760817$
	3rd (even)	$\pm 3.859206 - i1.026413$	$6.919976 \mp i3.961141$
	4th (odd)	$\pm 5.434003 - i1.196991$	$14.047800 \mp i6.504453$
3.5	1st (even)	$\pm 0.128122 - i0.631865$	$-0.191419 \mp i0.080956$
	2nd (odd)	$\pm 2.081119 - i1.419230$	$1.158421 \mp i2.953588$
	3rd (even)	$\pm 3.732794 - i1.670234$	$5.572035 \mp i6.234640$
	4th (odd)	$\pm 5.344483 - i1.834867$	$12.598384 \mp i9.806418$
4	1st (odd)	$\pm 2.063480 - i1.492993$	$1.014461 \mp i3.080762$
	2nd (even)	$\pm 3.722309 - i1.740012$	$5.413971 \mp i6.476865$
	3rd (odd)	$\pm 5.336963 - i1.903372$	$12.430178 \mp i10.158227$
10	1st (odd)	$\pm 1.964311 - i2.007908$	$-0.086589 \mp i3.944158$
	2nd (even)	$\pm 3.659154 - i2.221936$	$4.226203 \mp i8.130410$
	3rd (odd)	$\pm 5.290767 - i2.374988$	$11.175823 \mp i12.565511$

that Eq. (3·22) gives

$$\varepsilon_n = \frac{\hbar^2}{2m}(k_n^2 - \kappa_n^2) \quad \text{and} \tag{3·23}$$

$$\Gamma_n = \frac{2\hbar^2}{m} k_n \kappa_n. \tag{3·24}$$

The latter equation is equivalent to Eq. (2·15). Since we always have

$$-\kappa_n \equiv \mathrm{Im}\, K_n < 0, \tag{3·25}$$

we also have $\mathrm{Im}\, E_n < 0$, or

$$\Gamma_n > 0 \quad \text{for the solutions with } k_n > 0. \tag{3·26}$$

This reveals that states with outgoing waves only are indeed decaying. For solutions with $k_n < 0$, contrastingly, we have $\mathrm{Im}\, E_n > 0$, or

$$\Gamma_n < 0 \quad \text{for the solutions with } k_n < 0. \tag{3·27}$$

This reveals that such states grow because of the incoming waves; such states are often called anti-resonant states. We discuss these facts further in §4.

Decaying resonant states and growing anti-resonant states always appear in pairs. Both such states break time-reversal symmetry;[57)–59)] the latter states are the time-reversed states of the former.

3.3. *Relation to the S matrix*

Let us now demonstrate for the double delta potential (3·11) that the pole of the S matrix also gives the results in Table I. Computing the S matrix, or computing the transmission and reflection amplitudes, differs from the computation given in §3.2 with respect to two points. First, the wave function assumes the form

$$\psi(x) = \begin{cases} Ae^{iKx} + Be^{-iKx} & \text{for } x < -l, \\ Fe^{iKx} + Ge^{-iKx} & \text{for } -l < x < l, \\ Ce^{iKx} & \text{for } x > l, \end{cases} \tag{3·28}$$

rather than that appearing in Eq. (3·12). Second, the wave number K (and hence the energy eigenvalue E) is a given real number. (Below, we carry out its analytic continuation onto the complex K plane.) The undetermined constants here are the four ratios of the coefficients A, B, C, F, and G, while we have four connection conditions, Eqs. (3·13)–(3·14). Hence, the four ratios can be obtained as functions of K. We can rephrase this point as follows: We have five undetermined constants, the wave number K and the four ratios, whereas we have only four conditions, and hence there is a continuous set of solutions on the real K axis.

The connection conditions (3·13)–(3·14) relate the five coefficients as

$$\begin{pmatrix} e^{-iKl} & e^{iKl} \\ (iK + a^{-1})e^{-iKl} & -(iK - a^{-1})e^{iKl} \end{pmatrix} \begin{pmatrix} A \\ B \end{pmatrix} = \begin{pmatrix} e^{-iKl} & e^{iKl} \\ iKe^{-iKl} & -iKe^{iKl} \end{pmatrix} \begin{pmatrix} F \\ G \end{pmatrix}, \tag{3·29}$$

$$\begin{pmatrix} e^{iKl} & e^{-iKl} \\ iKe^{iKl} & -iKe^{-iKl} \end{pmatrix} \begin{pmatrix} F \\ G \end{pmatrix} = \begin{pmatrix} e^{iKl} \\ (iK - a^{-1})e^{iKl} \end{pmatrix} C. \tag{3·30}$$

By eliminating the vector $\begin{pmatrix} F \\ G \end{pmatrix}$, we have

$$\begin{pmatrix} A \\ B \end{pmatrix} = \frac{-1}{4K^2a^2} \begin{pmatrix} (2iKa-1)^2 - e^{4iKl} \\ (2iKa-1)e^{-2iKl} + (2iKa+1)e^{2iKl} \end{pmatrix} C. \tag{3·31}$$

The S matrix is then given by

$$S(K) = \begin{pmatrix} r(K) & t(K) \\ t(K) & r(K) \end{pmatrix}, \tag{3·32}$$

with

$$r(K) \equiv \frac{B}{A} = \frac{4iKa\cos 2Kl + 2i\sin 2Kl}{(2iKa-1)^2 - e^{4iKl}}, \tag{3·33}$$

$$t(K) \equiv \frac{C}{A} = \frac{-4K^2a^2}{(2iKa-1)^2 - e^{4iKl}}. \tag{3·34}$$

Now we carry out the analytic continuation onto the complex K plane. The poles of the elements of the S matrix are determined by the zeros of the denominator,

$$(2iKa-1)^2 - e^{4iKl} = 0. \tag{3·35}$$

This equation is equivalent to Eq. (3·17) in §3.2. It is notable, however, that the parity of the eigenstate is not obtained from the S matrix.

Note that in Eq. (3·31) the coefficient A vanishes at the complex zeros of Eq. (3·35), and the wave function (3·28) reduces to the resonant wave function (3·12). (The flux is conserved only when K is real.) Thus we have shown that the solutions given in Table I are identical to the resonant states obtained with the indirect method of definition.

The transmission probability $T \equiv |t(K)|^2$ has "resonance peaks" on the real k axis (and on the real ε axis) as the skirts of the poles of the function $t(K)$. In Fig. 4, we have superimposed the locations of the resonant states on the k dependence of the transmission probability T. A resonant state with a small imaginary part yields a resonance peak near its real part, but a resonant state with a large imaginary part and the corresponding resonance peak are separated by a greater distance.

Note that in Figs. 4(d) and (e), the first "resonance peak" does not have a corresponding resonant state, as mentioned in §3.2; perhaps we should not call this peak a "resonance peak".

§4. Diverging eigenfunctions and particle-number conservation

Following the above example, we now discuss the resonant wave function in the general case. We first show that a resonant eigenfunction is diverging away from the scattering potential. In spite of, or rather, thanks to the divergence, the resonant wave function indeed conserves the particle number.

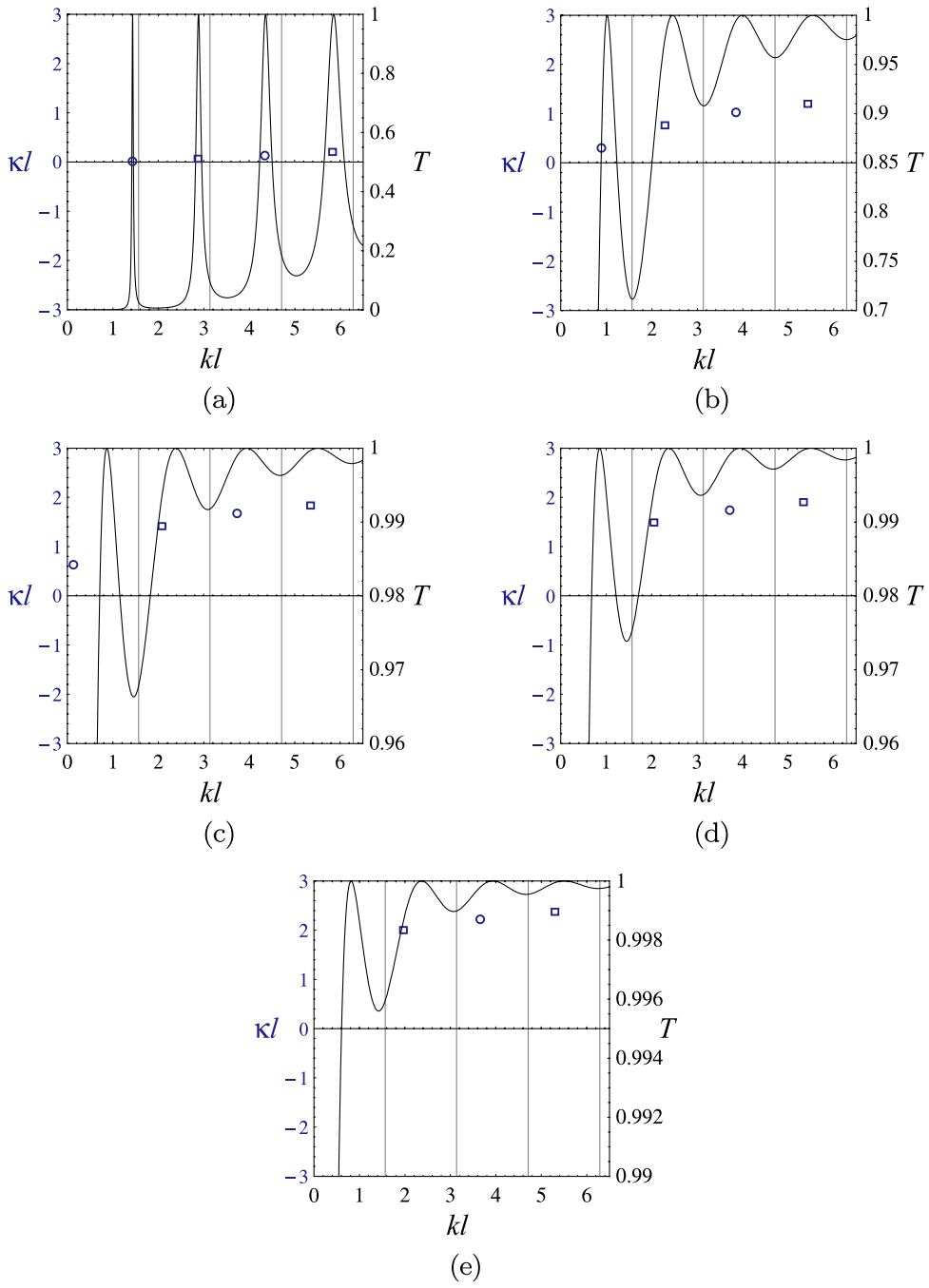

Fig. 4. The k dependence of the transmission probability T (the right axis of each panel) in the cases (a) $a/l = 0.1$, (b) $a/l = 1$, (c) $a/l = 3.5$, (d) $a/l = 4$, and (e) $a/l = 10$. The vertical thin gray lines indicate $kl = n\pi$. The locations of the resonant states given in Fig. 3 are superimposed (the left axis of each panel). (The circles indicate the even solutions and the squares indicate the odd solutions.) Note that in (d) and (e), the first "resonance" peak does not have a corresponding resonance pole.

4.1. *Divergence of the resonant eigenfunction*

The general form of the one-dimensional resonant wave function (3·3) now reads

$$\psi_{\mathrm{res},n}(x) = \begin{cases} Be^{-ik_n x - \kappa_n x} & \text{for } x < -L, \\ Ce^{ik_n x + \kappa_n x} & \text{for } x > L. \end{cases} \tag{4·1}$$

We argue in the following that the above eigenfunction is diverging away from the potential.

The solution (4·1) is an eigenfunction of the stationary Schrödinger equation under the boundary conditions such that there exist only the outgoing waves:

$$\hat{\mathcal{H}}\psi_{\mathrm{res},n} = \left(\varepsilon_n - i\frac{\Gamma_n}{2}\right)\psi_{\mathrm{res},n}. \tag{4·2}$$

The solution of the time-dependent Schrödinger equation (2·16) is then given by

$$\Psi_{\mathrm{res},n}(x,t) = \psi_{\mathrm{res},n}(x)\exp\left[-\frac{i}{\hbar}\left(\varepsilon_n - i\frac{\Gamma_n}{2}\right)t\right]. \tag{4·3}$$

Then the particle number of this particular state in the segment Ω,

$$N_{n,\Omega}(t) \equiv \langle \Psi_{\mathrm{res},n} | \Psi_{\mathrm{res},n} \rangle_\Omega, \tag{4·4}$$

decays as in Eq. (2·18), or

$$\begin{aligned} \frac{d}{dt}N_{n,\Omega}(t) &= -e^{-\Gamma_n t/\hbar} \times \frac{\Gamma_n}{\hbar}\langle \psi_{\mathrm{res},n} | \psi_{\mathrm{res},n} \rangle_\Omega \\ &= -e^{-\Gamma_n t/\hbar} \times \frac{\Gamma_n}{\hbar} N_{n,\Omega}(0). \end{aligned} \tag{4·5}$$

If the eigenfunction has outgoing waves only, or $k_n \equiv \mathrm{Re}\, K_n > 0$, then the state should decay in time, or $\Gamma_n > 0$, because particles leak from the central segment Ω. If the eigenfunction satisfies $k_n < 0$, on the other hand, the state should grow in time, or $\Gamma_n < 0$, because particles flow into the central segment Ω. As illustrated in §3.2, and particularly in Eqs. (3·23)–(3·26), the above physical conditions,

$$k_n > 0 \Leftrightarrow \Gamma_n > 0, \tag{4·6}$$

$$k_n < 0 \Leftrightarrow \Gamma_n < 0, \tag{4·7}$$

are necessary and sufficient conditions for

$$\kappa_n \equiv -\,\mathrm{Im}\, K_n > 0, \tag{4·8}$$

owing to the exact relation (2·15), or (3·24):

$$\Gamma_n = \frac{2\hbar^2}{m} k_n \kappa_n. \tag{4·9}$$

Upon applying the inequality (4·8) to the wave function (4·1), we realize that the resonant eigenfunction must diverge as $|x| \to \infty$.

We can also show the necessity of the divergence of the resonant eigenfunction (4·1) through the following dimensional analysis. For the eigenfunction (4·1), the formula (2·12) reads

$$\frac{\Gamma_n}{2}\langle\psi_{\mathrm{res},n}|\psi_{\mathrm{res},n}\rangle_{\Omega} = \frac{\hbar^2 k_n}{2m}\langle\psi_{\mathrm{res},n}|\psi_{\mathrm{res},n}\rangle_{\partial\Omega}. \tag{4·10}$$

As we expand the volume of the integration, Ω, the left-hand side of Eq. (4·10) would increase in proportion to the volume of the region, $|\Omega|$, whereas the right-hand side would increase in proportion to $|\Omega|^{(d-1)/d}$, where d is the dimensionality of the space. This apparent inconsistency results from the implicit assumption that the wave function is almost constant over the volume of the integration. This inconsistency is avoided if the wave function in Eq. (4·10) grows or decays exponentially as we expand the integration volume Ω.

Indeed, the solution (4·1) gives the left-hand side of the formula (4·10) as

$$\frac{\Gamma_n}{2}\langle\psi_{\mathrm{res},n}|\psi_{\mathrm{res},n}\rangle_{\Omega} \simeq \frac{\Gamma_n}{2}\int_{-L}^{L} e^{2\kappa_n|x|}dx = \frac{\Gamma_n}{2\kappa_n}e^{2\kappa_n L}, \tag{4·11}$$

where we have ignored the details of the wave function around the origin. Also, the solution (4·1) gives the right-hand side of the formula (4·10) as

$$\frac{\hbar^2 k_n}{2m}\langle\psi_{\mathrm{res},n}|\psi_{\mathrm{res},n}\rangle_{\partial\Omega} = \frac{\hbar^2 k_n}{m}e^{2\kappa_n L}. \tag{4·12}$$

These two expressions are equal because of the relation (4·9). (In fact, it is customary to normalize the diverging wave function by first introducing a Gaussian convergence factor $\exp(-\alpha x^2)$ in the volume integration in Eq. (4·11) and then, after integration, setting α to 0.[5)] This gives the normalization factor $1/\sqrt{2\kappa_n}$ for the eigenfunction.)

Thus, here we characterize the resonant state as *an eigenfunction taking the form of an exponentially divergent outgoing wave and an eigenvalue with a negative imaginary part*. We show in the next subsection that this divergence is physically plausible; the resonant eigenfunction must diverge in order for the particle number to be conserved. The method for treating the divergence is also a central issue studied in §§5 and 6; we propose methods for eliminating the divergence computationally in §§5 and 6.

4.2. *Particle number conservation*

Here we show that we can intuitively understand the divergence of the resonant eigenfunction from the point of view of particle number conservation. Because the energy eigenvalue is complex, the particle number is not conserved in the conventional sense. We show that the particle number in a volume that expands in time is indeed conserved. We then show that the resonant eigenfunction must be diverging in order to conserve the particle number.

As we show in Fig. 2, the number of particles in the trapping potential decreases because some of the particles escape the potential. The particles that escape move with a velocity of $\hbar k_n/m$. The idea here is to count the particle number in a volume

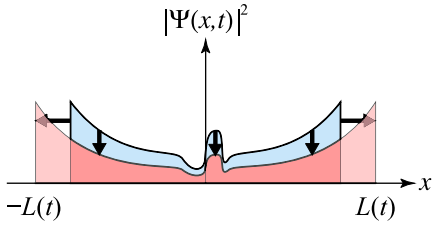

Fig. 5. The wave amplitude decreases exponentially at every point, whereas it increases exponentially as $|x| \to \infty$. The integral is constant.

that expands at the same velocity; in the simple one-dimensional case, for example, we make the boundary L move as

$$L(t) = \frac{\hbar k_n}{m} t. \tag{4·13}$$

Then the particle number included in the expanding volume $\Omega(t)$ should be conserved.

We can estimate the particle number (4·4) as

$$\begin{aligned} N_{n,\Omega(t)}(t) &= e^{-\Gamma_n t/\hbar} \int_{-L(t)}^{L(t)} |\psi_{\mathrm{res},n}|^2 \, dx \\ &\simeq e^{-\Gamma_n t/\hbar} \times \frac{1}{\kappa_n} e^{2\kappa_n L(t)} \\ &= \frac{1}{\kappa_n} \exp\left[\left(-\frac{\Gamma_n}{\hbar} + \frac{2\hbar k_n \kappa_n}{m}\right) t\right], \end{aligned} \tag{4·14}$$

where we have ignored the details of the wave function around the origin. The right-hand side of Eq. (4·14) is indeed constant, because of the relation (4·9). The exponential temporal decrease of the wave amplitude is cancelled by its exponential spatial increase (Fig. 5).

In short, the divergence of the resonant eigenfunction indicates that the particle eventually escapes to infinity. Thus, the divergence is not simply plausible but necessary for the particle number to be conserved.

We note that the edge of the expanding volume is well-defined and never spreads, in spite of the fact that we have a nonlinear dispersion relation, $E = \hbar^2 K^2/2m$. This is because here we are considering properties of a single resonant state, and hence we are not considering the spreading of an arbitrary wave packet.

§5. Numerical method for finding resonant eigenvalues

As argued in §4, the eigenfunction of the resonant state necessarily diverges away from the scattering potential. This divergence can make it difficult to treat resonant states numerically within the framework of the direct method of defining the resonant state. The resonant state would disappear if we naively truncate the infinite space in numerical calculations. A conventional method for avoiding this difficulty

in the framework of the direct method is to suppress the divergence by employing complex scaling, or complex rotation.[14)–16),30),44)–53)] The complex rotation modifies the Hamiltonian according to

$$\hat{p} \to \hat{p}(\theta) \equiv \hat{p}e^{-i\theta}, \tag{5·1}$$

$$x \to x(\theta) \equiv xe^{i\theta}. \tag{5·2}$$

Modification of the momentum operator, given in Eq. (5·1), causes the resonant eigenfunctions to be in the L^2 functional space. Modification of the coordinate operator, given in Eq. (5·2), which must be introduced to conserve the commutation relation, can be problematic, however. The potential $V(x)$ must be an analytic function in order for the modification (5·2) to be applied;[14)–16)] we cannot apply complex scaling to a box potential nor to any lattice models. When the potential $V(x)$ is a Gaussian scattering potential, complex scaling is applicable only for $\theta < \pi/4$; otherwise, the potential becomes divergent.

This problem can be avoided in some cases by extending the complex scaling method. In the exterior complex scaling,[60),61)] the coordinate operator is modified as

$$x \to \begin{cases} x & \text{for } |x| \le R_0, \\ R_0 + (|x| - R_0)e^{i\theta} & \text{for } |x| > R_0, \end{cases} \tag{5·3}$$

where R_0 is a constant. Non-analyticity of the potential in the region $|x| \le R_0$ is thus allowed. However, this method may still be inapplicable to lattice models.

In the present section, we propose a new numerical method for finding resonant eigenvalues iteratively in the complex energy plane. Our method is independent of the complex scaling and free from the above restrictions; in fact, we demonstrate the method for a lattice model. We hence believe that the present method is particularly useful in condensed matter physics. The method utilizes an effective potential,[31)–42)] which is called the self-energy of the leads in the context of condensed matter physics. This effective potential is actually an energy-dependent boundary condition and is useful for truncating the infinite space of an open system.

The resonant eigenvalue is obtained exactly once the energy-dependent effective potential is fixed exactly. To fix the effective potential exactly, however, we need to know the resonant eigenvalue exactly. In other words, the resonant eigenvalue and the effective potential must be self-consistent. We make the postulated value of the eigenvalue converge to the exact value by seeking self-consistency between the eigenvalue and the effective potential.

5.1. *Effective potential*

Before presenting our numerical method, let us introduce the effective potential, following Ref. 42). The effective potential was first introduced in nuclear physics half a century ago.[31)–34)] It has been occasionally used in studies of the physics of mesoscopic systems in recent years.[35)–42)]

We demonstrated in §3 that we can obtain the resonant eigenvalue using the boundary condition of purely outgoing waves. When the scattering potential is complicated, we may need to solve the Schrödinger equation numerically. Consider,

for simplicity, the Schrödinger equation in one dimension:

$$-\frac{\hbar^2}{2m}\frac{\partial^2}{\partial x^2}\psi(x) + V(x)\psi(x) = E\psi(x). \tag{5·4}$$

We solve this equation numerically by discretizing the x space with a grid size Δx. We then have

$$-\frac{t_{\rm h}}{2}\left(\psi(x-\Delta x) + \psi(x+\Delta x)\right) + V(x)\psi(x) = (E - t_{\rm h})\psi(x), \tag{5·5}$$

where

$$t_{\rm h} \equiv \frac{\hbar^2}{m(\Delta x)^2}. \tag{5·6}$$

In condensed matter physics, the same form of the Schrödinger equation appears from a different origin.[62] Consider a metal with a regular lattice of atoms with lattice constant Δx. Suppose that an orbital $\psi(x)$ of an atom overlaps the same orbital of the neighboring atom, $\psi(x+\Delta x)$. Then an electron can hop from atom to atom with an amplitude given by the overlap integral

$$t_{\rm h} \equiv \frac{\hbar^2}{m}\int \psi(x+\Delta x)\frac{\partial^2}{\partial x^2}\psi(x)dx. \tag{5·7}$$

This perturbational argument gives a Schrödinger equation of the same form as Eq. (5·5), except for the constant $t_{\rm h}$ on the right-hand side. This is called the tight-binding model, which may be relevant when the kinetic energy is much less than the atomic binding energy. We hereafter drop the constant $t_{\rm h}$ on the right-hand side by shifting the origin of the energy scale.

With the above consideration, we solve the equation

$$\begin{aligned}\hat{\mathcal{H}}\psi_{{\rm res},n}(x) &\equiv -\frac{t_{\rm h}}{2}\left(\psi_{{\rm res},n}(x-\Delta x) + \psi_{{\rm res},n}(x+\Delta x)\right) + V(x)\psi_{{\rm res},n}(x) \\ &= E_n\psi_{{\rm res},n}(x),\end{aligned} \tag{5·8}$$

to obtain the resonant eigenstates $\{\psi_{{\rm res},n}\}$. Suppose that we attempt to solve the Schrödinger equation in the finite region $-L \le x \le L$, which contains the support of the potential; in other words, the potential is zero at the boundaries and outside the region:

$$V(x) \equiv 0 \quad \text{for} \quad |x| \ge L. \tag{5·9}$$

Then, the resonant eigenfunction at the boundaries must contain the outgoing wave only:

$$\psi_{{\rm res},n}(x) \propto e^{iK_n|x|} \quad \text{for} \quad |x| \ge L. \tag{5·10}$$

Then, using the form (5·10) in the Schrödinger equation (5·8) in the region without the potential, we have

$$-\frac{t_{\rm h}}{2}\left(e^{iK_n|x+\Delta x|} + e^{iK_n|x-\Delta x|}\right) = E_n e^{iK_n|x|}. \tag{5·11}$$

We thus find that the wave number K_n is related to the eigenvalue E_n as

$$E_n = -t_{\rm h} \cos(K_n \Delta x), \tag{5·12}$$

where E_n and K_n are generally complex numbers. This dispersion relation is called the "cosine band" in condensed matter physics. It gives the usual non-relativistic dispersion relation, $E_n \sim {K_n}^2$, in the limit $\Delta x \to 0$. Note, however, that Δx is not a small number in the tight-binding model of condensed matter physics.

Here, we cast Eq. (5·10) into the form

$$\psi_{{\rm res},n} (\pm (L + \Delta x)) = e^{iK_n \Delta x} \psi_{{\rm res},n} (\pm L) \tag{5·13}$$

and substitute it for the term in Eq. (5·8) outside the region in question. We thus have

$$\begin{aligned} \hat{\mathcal{H}} \psi_{{\rm res},n} (\pm L) &= -\frac{t_{\rm h}}{2} \psi_{{\rm res},n} (\pm L - \Delta x) - \frac{t_{\rm h}}{2} \psi_{{\rm res},n} (\pm L + \Delta x) \\ &= -\frac{t_{\rm h}}{2} \psi_{{\rm res},n} (\pm (L - \Delta x)) + V_{{\rm eff},n} (\pm L) \psi_{{\rm res},n} (\pm L) \\ &= E_n \psi_{{\rm res},n} (\pm L), \end{aligned} \tag{5·14}$$

where the effective potential is given by

$$V_{{\rm eff},n} (\pm L) \equiv -\frac{t_{\rm h}}{2} e^{iK_n \Delta x}. \tag{5·15}$$

Using Eq. (5·12), this can be rewritten in terms of the energy eigenvalue as

$$V_{{\rm eff},n} (\pm L) = \frac{1}{2} \left(E_n - i \sqrt{{t_{\rm h}}^2 - {E_n}^2} \right), \tag{5·16}$$

where we have assumed ${\rm Re}\, K_n > 0$ in order to fix the sign of the imaginary part.

Equation (5·16) possesses the form often found in the literature (e.g., Refs. 35) and 40)), where the effective potential is obtained as the self-energy that comes into the energy denominator of the Green's function. The easier derivation appearing above is noted in Ref. 42).

The effective potential (5·16) is an energy-dependent complex potential; it is different for different resonant states. As a result, the Hamiltonian matrix [such as Eq. (5·36) below] with the effective potential is a non-Hermitian operator and may have a complex eigenvalue. The point here is that Eq. (5·14) contains only the eigenfunctions inside the region $-L \leq x \leq L$. Hence, we can solve the Schrödinger equation by restricting ourselves to the region in question.

5.2. *Self-consistent solution*

We now propose a numerical method for finding a resonant eigenvalue by utilizing the self-consistency of the resonant eigenvalue and the effective potential. This method starts with the postulate of a complex resonant eigenvalue, $E^{(0)}$. This gives the corresponding complex effective potential

$$V_{\rm eff}^{(0)} (\pm L) = \frac{1}{2} \left(E^{(0)} - i \sqrt{{t_{\rm h}}^2 - {E^{(0)}}^2} \right). \tag{5·17}$$

We can then diagonalize the Hamiltonian in the region $-L \le x \le L$ with the effective potential $V_{\rm eff}^{(0)}$. From the resulting eigenvalues, we choose the one closest to the postulated eigenvalue $E^{(0)}$ and refer to it as an updated postulated eigenvalue $E^{(1)}$. This, again, gives the corresponding effective potential $V_{\rm eff}^{(1)}$. We repeat the procedure of

1. obtaining an updated postulated eigenvalue $E^{(q)}$ from the diagonalization of the Hamiltonian with the effective potential $V_{\rm eff}^{(q-1)}$,
2. and determining the effective potential $V_{\rm eff}^{(q)}$ from the postulated eigenvalue $E^{(q)}$.

For the few simple examples that we have tested, the convergence of this method is surprisingly good, even with the above straightforward iteration. A more sophisticated iteration may be necessary in more complicated cases. In the following, we demonstrate that a straightforward iteration for a simple model Hamiltonian yields exponentially rapid convergence.

We solve the Schrödinger equation (5·8) with the potential

$$V(x) = \begin{cases} V_0 > 0 & \text{for } x = \pm \Delta x, \\ 0 & \text{otherwise.} \end{cases} \tag{5·18}$$

Let us first solve the problem exactly. As we showed in §3, we assume that the eigenfunction has outgoing waves only. We then have solutions with even parity and solutions with odd parity. Equations (3·3) and (3·16) show that we can assume the form

$$\psi_{{\rm res},n}(x) = \begin{cases} \pm B_n e^{-iK_n x} & \text{for } x \le -\Delta x, \\ F_n & \text{for } x = 0, \\ B_n e^{iK_n x} & \text{for } x \ge \Delta x, \end{cases} \tag{5·19}$$

where B_n and F_n are constant. The Schrödinger equation for $|x| > \Delta x$,

$$-\frac{t_{\rm h}}{2}\left(\psi_{{\rm res},n}(x-\Delta x) + \psi_{{\rm res},n}(x+\Delta x)\right) = E_n \psi_{{\rm res},n}(x), \tag{5·20}$$

gives the dispersion relation (5·12). The Schrödinger equation at $x = \Delta x$ and at $x = 0$ reads

$$-\frac{t_{\rm h}}{2}\left(\psi_{{\rm res},n}(0) + \psi_{{\rm res},n}(2\Delta x)\right) + V(1)\psi_{{\rm res},n}(\Delta x) = E_n \psi_{{\rm res},n}(\Delta x), \tag{5·21}$$

$$-\frac{t_{\rm h}}{2}\left(\psi_{{\rm res},n}(-\Delta x) + \psi_{{\rm res},n}(\Delta x)\right) = E_n \psi_{{\rm res},n}(0). \tag{5·22}$$

These two equations reduce to

$$-\left(F_n + B_n e^{2iK_n\Delta x}\right) + 2\tilde{V}_0 B_n e^{iK_n\Delta x} = -B_n e^{iK_n\Delta x}\left(e^{iK_n\Delta x} + e^{-iK_n\Delta x}\right), \tag{5·23}$$

$$-2B_n e^{iK_n\Delta x} = -F_n\left(e^{iK_n\Delta x} + e^{-iK_n\Delta x}\right) \quad \text{for even parity,} \tag{5·24}$$

$$0 = -F_n\left(e^{iK_n\Delta x} + e^{-iK_n\Delta x}\right) \quad \text{for odd parity,} \tag{5·25}$$

where $\tilde{V}_0 \equiv V_0/t_{\rm h}$, or

$$(2\tilde{V}_0 z_n + 1)B_n - F_n = 0, \tag{5·26}$$

$$2z_n B_n - (z_n + {z_n}^{-1})F_n = 0 \quad \text{for even parity,} \tag{5·27}$$

$$F_n = 0 \quad \text{for odd parity,} \tag{5·28}$$

where $z_n \equiv e^{iK_n \Delta x}$. For odd parity, we have the solution

$$z_n = -\frac{1}{2\tilde{V}_0}, \quad \text{or} \tag{5·29}$$

$$K_n \Delta x = \pi + i \log 2\tilde{V}_0 \quad \text{and} \quad E_n = \tilde{V}_0 + \frac{1}{4\tilde{V}_0}, \tag{5·30}$$

which is a bound state with real energy. For even parity, we eliminate the degree of freedom of B_n/F_n, arriving at the third-order equation

$$2\tilde{V}_0 {z_n}^3 - {z_n}^2 + 2\tilde{V}_0 z_n + 1 = 0. \tag{5·31}$$

The three solutions for $\tilde{V}_0 = 1$, for example, are

$$E_n/t_{\rm h} = 1.517526485679543\ldots, \tag{5·32}$$

$$E_n/t_{\rm h} = -0.383763242839771\ldots - i0.132164836187054\ldots \tag{5·33}$$

$$E_n/t_{\rm h} = -0.383763242839771\ldots + i0.132164836187054\ldots \tag{5·34}$$

The first solution is another bound state. The second solution is a resonant state, and the third solution an anti-resonant state.

These are the exact solutions with real and complex energy eigenvalues. We now demonstrate our numerical iterative method with rapid convergence to obtain the resonant state with a complex eigenvalue.

In order to choose the first postulated eigenvalue, it may be useful to consider the quantity

$$D(E) = |\det\left(\mathcal{H}_{\rm eff}(E) - EI\right)| \tag{5·35}$$

in the complex E plane, where the effective Hamiltonian $\mathcal{H}_{\rm eff}(E)$ is defined on the region $-L \le x \le L$ with the effective potential. We hereafter set $L = 2$, for example. We then have

$$\mathcal{H}_{\rm eff}(E) = \begin{pmatrix} V_{\rm eff}(E) & -\frac{t_{\rm h}}{2} & 0 & 0 & 0 \\ -\frac{t_{\rm h}}{2} & V_0 & -\frac{t_{\rm h}}{2} & 0 & 0 \\ 0 & -\frac{t_{\rm h}}{2} & 0 & -\frac{t_{\rm h}}{2} & 0 \\ 0 & 0 & -\frac{t_{\rm h}}{2} & V_0 & -\frac{t_{\rm h}}{2} \\ 0 & 0 & 0 & -\frac{t_{\rm h}}{2} & V_{\rm eff}(E) \end{pmatrix}, \tag{5·36}$$

where

$$V_{\rm eff}(E) \equiv \frac{1}{2}\left(E - i\sqrt{{t_{\rm h}}^2 - E^2}\right). \tag{5·37}$$

The zeros of $D(E)$ correspond to the eigenvalues, although it is not practical to use the zeros as numerical estimators of the eigenvalues. Figure 6 displays a three-dimensional plot of $\log|D(E)|$ in the complex energy plane. The dimple in the lower left corner is the resonance pole given in Eq. (5·33).

On the basis of the rough estimation given in Fig. 6, we choose the first postulated eigenvalue as $E^{(0)} = -0.3 - i0.1$. The postulated eigenvalue $E^{(q)}$ converges to the eigenvalue (5·33) exponentially quickly with respect to the number of iterations, q (see Fig. 7). The numerical calculation involves diagonalization of 5×5 non-Hermitian matrices.

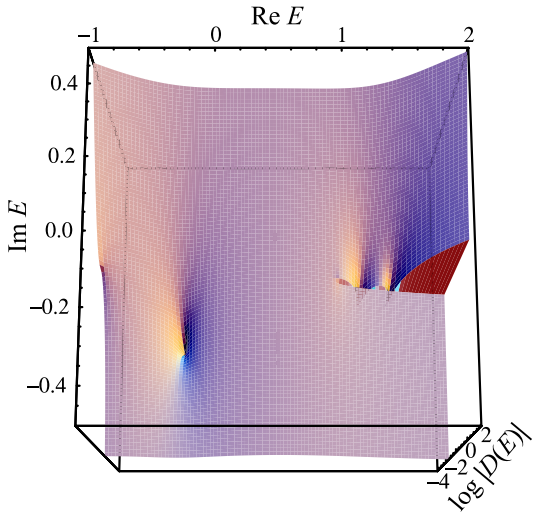

Fig. 6. A three-dimensional plot of $\log|D(E)|$ in the complex energy plane.

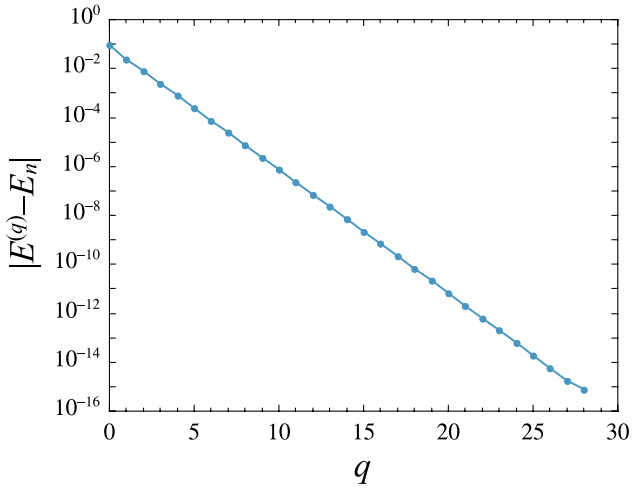

Fig. 7. Convergence of the numerical procedure proposed here for the model (5·18) with $V_0/t_h = 1$. The postulated eigenvalue $E^{(q)}$ approaches the exact value exponentially quickly with respect to the step number q.

§6. Numerical computation of the dynamics of resonant eigenfunctions

We finally introduce a trick for the numerical computation of the dynamics of diverging resonant eigenfunctions using the effective potential defined given in §5.1. The trick introduced below enables us to calculate the time evolution of the divergent eigenfunction precisely in a finite space when we discretize the space for the numerical calculation or when we consider a tight-binding model, as in Eq. (5·5).

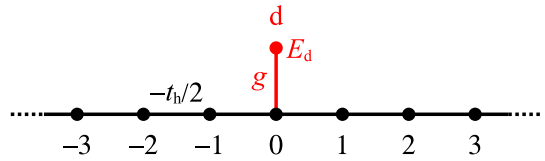

Fig. 8. The tight-binding model on a chain with an adatom.

Now, we are interested in integrating the time-dependent Schrödinger equation

$$i\hbar\frac{\partial}{\partial t}\Psi_{\mathrm{res},n}(x,t)=\hat{\mathcal{H}}\Psi_{\mathrm{res},n}(x,t), \tag{6·1}$$

where the Hamiltonian $\hat{\mathcal{H}}$ is given in Eq. (5·8). On the right-hand side, we again eliminate the region $|x|>L$, as in Eq. (5·14), with the use of the following effective potential:

$$\hat{\mathcal{H}}\Psi_{\mathrm{res},n}\left(\pm L,t\right)=-\frac{t_{\mathrm{h}}}{2}\Psi_{\mathrm{res},n}\left(\pm\left(L-\Delta x\right),t\right)+V_{\mathrm{eff},n}\left(\pm L\right)\Psi_{\mathrm{res},n}\left(\pm L,t\right). \tag{6·2}$$

Because we already know the energy eigenvalues from the method presented in §5, we can fix the effective potential $V_{\mathrm{eff},n}\left(\pm L\right)$ for each resonant state. The point here is that Eq. (6·2) contains only the eigenfunctions inside the region $-L\leq x\leq L$. Hence we can integrate Eq. (6·1) by restricting ourselves to the region in question.

Let us demonstrate the above trick with the computation of a version of the Friedrichs-Fano (or Newns-Anderson) model (Fig. 8):[64)–67)]

$$\hat{\mathcal{H}}=-\frac{t_{\mathrm{h}}}{2}\sum_{x}\left(\left|x+\Delta x\right\rangle\left\langle x\right|+\left|x\right\rangle\left\langle x+\Delta x\right|\right)+g\left(\left|\mathrm{d}\right\rangle\left\langle 0\right|+\left|0\right\rangle\left\langle \mathrm{d}\right|\right)+E_{\mathrm{d}}\left|\mathrm{d}\right\rangle\left\langle \mathrm{d}\right|, \tag{6·3}$$

where d denotes the site of an adatom. The first term represents the tight-binding hopping on a chain, the second term represents the hopping between the origin of the chain $x=0$ and the adatom, and the third term represents the impurity level of the adatom.

Let us first find the resonance poles exactly. As we showed in §3, we assume that the eigenfunction has outgoing waves only. We then have solutions with even parity and solutions with odd parity. The odd solutions vanish at $x=0$, and hence do not couple to the adatom. We consider only even solutions hereafter. We assume the form

$$\psi_{\mathrm{res},n}(x)=B_n e^{iK_n|x|} \tag{6·4}$$

for the chain and

$$\psi_{\mathrm{res},n}(\mathrm{d})=F_n \tag{6·5}$$

for the adatom. The same procedure as in §5.2 yields the fourth-order equation

$$z_n{}^4+2\tilde{E}_{\mathrm{d}}z_n{}^3+4\tilde{g}^2z_n{}^2-2\tilde{E}_{\mathrm{d}}z_n-1=0, \tag{6·6}$$

where $z_n=e^{iK_n\Delta x}$, $\tilde{E}_{\mathrm{d}}\equiv E_{\mathrm{d}}/t_{\mathrm{h}}$ and $\tilde{g}\equiv g/t_{\mathrm{h}}$. Hence, there are four solutions, as shown in Fig. 9, for $\tilde{g}=0.1$.

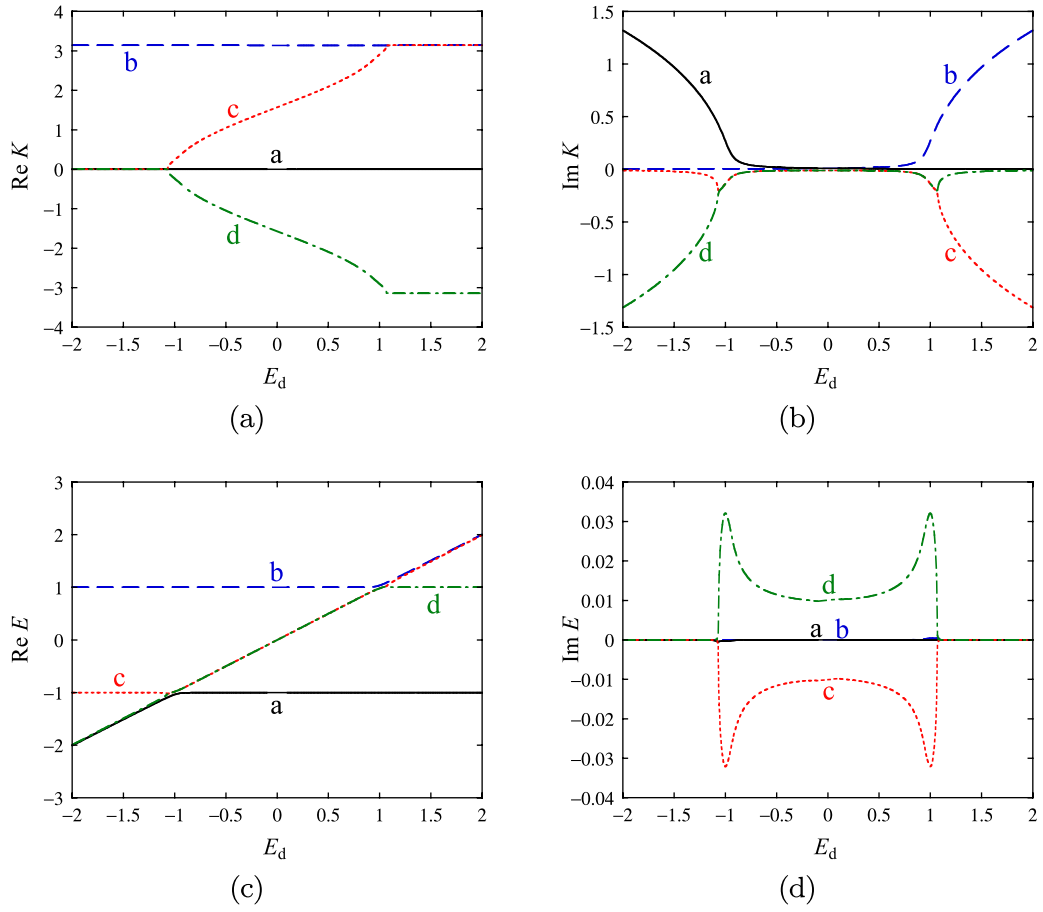

Fig. 9. The four solutions of Eq. (6·6) for $\tilde{g} = 0.1$. The dependence on the impurity level of (a) and (b) the real part and the imaginary part of $\{K_n\}$, respectively, and (c) and (d) the real part and the imaginary part of $\{\tilde{E}_n\}$, respectively, for $\tilde{g} = 0.1$. In each panel, the solid curve a and the broken curve b indicate bound states, while the dotted curve c and the long-short dashed curve d indicate resonant states.

Through the dispersion relation $E_n = -t_{\rm h}\cos(K_n \Delta x)$, or the relations

$$t_{\rm h}\left(z_n + \frac{1}{z_n}\right) = -2E_n, \tag{6·7}$$

$$t_{\rm h}\left(z_n - \frac{1}{z_n}\right) = \pm 2\sqrt{{E_n}^2 - {t_{\rm h}}^2}, \tag{6·8}$$

$${t_{\rm h}}^2\left({z_n}^2 - \frac{1}{{z_n}^2}\right) = \mp 4E_n\sqrt{{E_n}^2 - {t_{\rm h}}^2}, \tag{6·9}$$

the fourth-order equation (6·6) is transformed to an equation with respect to the energy:

$$\pm\left(E_n - E_{\rm d}\right)\sqrt{{E_n}^2 - {t_{\rm h}}^2} = g^2. \tag{6·10}$$

This is equivalent to the dispersion equation obtained in Ref. 67) for the Friedrichs

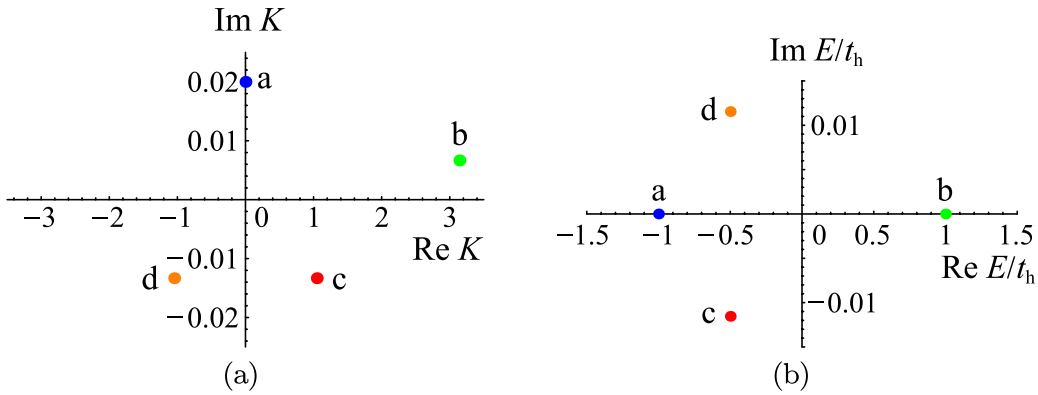

Fig. 10. The four solutions for $\tilde{g} = 0.1$ and $\tilde{E}_{\rm d} = -1/2$ in the complex momentum plane (a) and the complex energy plane (b). In each panel, the symbols a, b, c and d indicate the solutions represented by the solid curve, the broken curve, the dotted curve and the long-short dashed curve in Fig. 9, respectively. The solutions a and b are bound states, while the solutions c and d are resonant states.

model; see the pole of Eq. (7) in that paper. (The correspondence between the two notations is as follows: $E_n \Leftrightarrow z$, $E_{\rm d} \Leftrightarrow E_0$, $t_{\rm h} \Leftrightarrow B$, $g \Leftrightarrow gB$.) We stress that the equation is easier to obtain in momentum space than in energy space, because we need not perform a complicated integration of the self-energy part in the former case.

Two of the solutions (represented by the solid and broken curves, a and b, in Fig. 9) are bound states (positive $\mathrm{Im}\, K_n$ and real E_n) in the entire range and are referred to as "superstable states" in Ref. 67). The other two solutions (represented by the dotted and long-short dashed curves, c and d, in Fig. 9) have negative $\mathrm{Im}\, K_n$, which indicates that they are resonant states; more precisely, the state c is a resonant state with $\mathrm{Re}\, K > 0$ and the state d is the corresponding anti-resonant state with $\mathrm{Re}\, K < 0$. In some regions, the pair consisting of the resonant and anti-resonant states collide to form purely imaginary solutions, and hence the energy eigenvalues are real. States with purely imaginary wave numbers are often called anti-bound states,[63] but here we include them in resonant states.

Figure 10 plots the four solutions for $\tilde{g} = 0.1$ and $\tilde{E}_{\rm d} = -1/2$ in the complex momentum plane and the complex energy plane. The two solutions a and b are bound states. The solution a satisfies $\mathrm{Re}\, K_n = \pi$, and the solution b satisfies $\mathrm{Re}\, K_n = 0$. They are both on the first (the so-called *physical*) Riemann sheet of the complex energy plane. The other two solutions are resonant states. The solution c satisfies $\mathrm{Re}\, K_n > 0$ and $\mathrm{Im}\, E_n < 0$; this is a decaying resonant state with an outgoing wave only. The solution d satisfies $\mathrm{Re}\, K_n < 0$ and $\mathrm{Im}\, E_n > 0$; this is a growing anti-resonant state with an incoming wave only. These two are conjugate to each other and always appear in a pair, as demonstrated in §3.2. They are both on the second (the so-called *unphysical*) Riemann sheet of the complex energy plane.

We stress here again that it is generally more convenient to solve the problem in the complex momentum plane than in the complex energy plane. This is because of the added complexity involved in identifying the Riemann sheet for a given solution

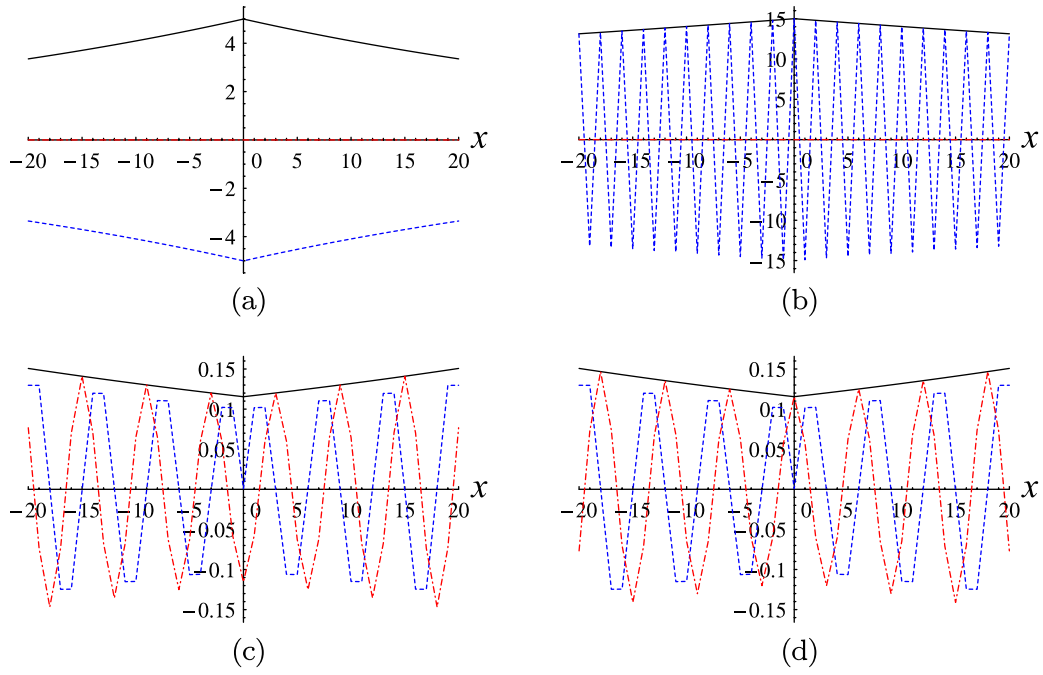

Fig. 11. The eigenfunctions at $t = 0$ for $\tilde{g} = 0.1$ and $\tilde{E}_{\rm d} = -1/2$: each panel displays the solution corresponding to, from top to bottom, the solid curve, the broken curve, the dotted curve and the long-short dashed curve in Fig. 9, or the solutions a, b, c and d in Fig. 10. The solutions a and b are bound states, while the solutions c and d are a pair consisting of a resonant state and an anti-resonant state. In each panel, the absolute value (the solid curve), the real part (the broken curve) and the imaginary part (the long-short dashed curve) are displayed in the region $-20 \leq x \leq 20$. (In the first and second panels, the imaginary part is zero.)

of the complex energy eigenvalue in the case that there are several Riemann sheets. It is generally not easy to tell whether a state is on the first or the second Riemann sheet before we determine the location of the state in the complex momentum plane.

The eigenfunctions $\{\psi_{{\rm res},n}(x)\}$ of the solutions a, b, c and d for $\tilde{g} = 0.1$ and $\tilde{E}_{\rm d} = -1/2$ are displayed in Fig. 11, where the normalization is always fixed by $\psi_{{\rm res},n}(d) = 1$. The eigenfunctions from (a) to (d) of Fig. 11 correspond to the solutions a, b, c and d in Fig. 10, respectively. It is evident that the solutions a and b are bound states decaying in space, whereas the solutions c and d are, respectively, resonant and anti-resonant states diverging in space.

We next solved the time-dependent Schrödinger equation

$$i\hbar\frac{\partial}{\partial t}\Psi_{{\rm res},n}(x,t) = \hat{\mathcal{H}}_{\rm eff}\Psi_{{\rm res},n}(x,t)$$

$$= \begin{cases} -\dfrac{t_{\rm h}}{2}\Psi_{{\rm res},n}(x+\Delta x,t) + V_{{\rm eff},n}\Psi_{{\rm res},n}(x,t) & \text{for } x=-L \\ -\dfrac{t_{\rm h}}{2}\left(\Psi_{{\rm res},n}(x-\Delta x,t)+\Psi_{{\rm res},n}(x+\Delta x,t)\right) + V(x)\Psi_{{\rm res},n}(x,t) & \text{for } -L<x<L \\ -\dfrac{t_{\rm h}}{2}\Psi_{{\rm res},n}(x-\Delta x,t) + V_{{\rm eff},n}\Psi_{{\rm res},n}(x,t) & \text{for } x=L \end{cases} \tag{6·11}$$

in the range $-L \le x \le L$ using the Runge-Kutta method, taking the eigenfunctions $\{\psi_{{\rm res},n}(x)\}$ as the initial conditions. The time evolution is partly shown in Fig. 12 for $\tilde{g}=0.1$ and $\tilde{E}_{\rm d}=-1/2$. The bound states a and b (the first and the second rows in Fig. 12) are time independent and stable, while the resonant state c in the third row decays in time, and the anti-resonant state d in the fourth row grows exponentially in time. It should be emphasized that if we had solved the original Schrödinger equation simply by truncating the domain of x without introducing the effective potential, we would not have obtained such accurate numerical results as in Figs. 11 and 12. This is especially true for the resonant eigenstates with complex eigenvalues, which diverge as $|x| \to \infty$.

We have applied the above technique to a more complicated model on a ladder lattice.[43] As a result, we have found a quasi-stable resonant state with a very long lifetime for quite a wide range of parameter values. This state appears to be a bound state around the impurity, diverging only far away from the scattering center, and barely decays for quite a long time. This finding is reported elsewhere.[43]

§7. Summary

In this paper, we have presented some properties of resonant states of open quantum systems in two parts. In the first part, we mostly reviewed the properties of quantum mechanical resonant states, but we also included two new points: (i) that the imaginary part of the energy expectation value is proportional to the momentum flux going out of the system for *arbitrary* wave functions; and (ii) that the number of particles in a resonant state is *conserved* when we count the number in an expanding volume. We also gave an example in which the "resonance peak" of the conductance is not accompanied by a resonant state.

In the second part, we presented numerical methods for finding a resonant state and computing its dynamics, using the effective Hamiltonian. This method for finding a resonance pole is independent of the complex scaling and is applicable to singular potentials as well as lattice models. This method is very efficient, exhibiting rapid convergence to the exact solution. The method of computing the time evolution of the divergent resonant eigenfunctions was demonstrated for the Friedrichs-Fano model.

We have intentionally avoided discussing the completeness relation and the resonant-state expansion.[68)–75)] We are planning to report studies of these topics elsewhere.

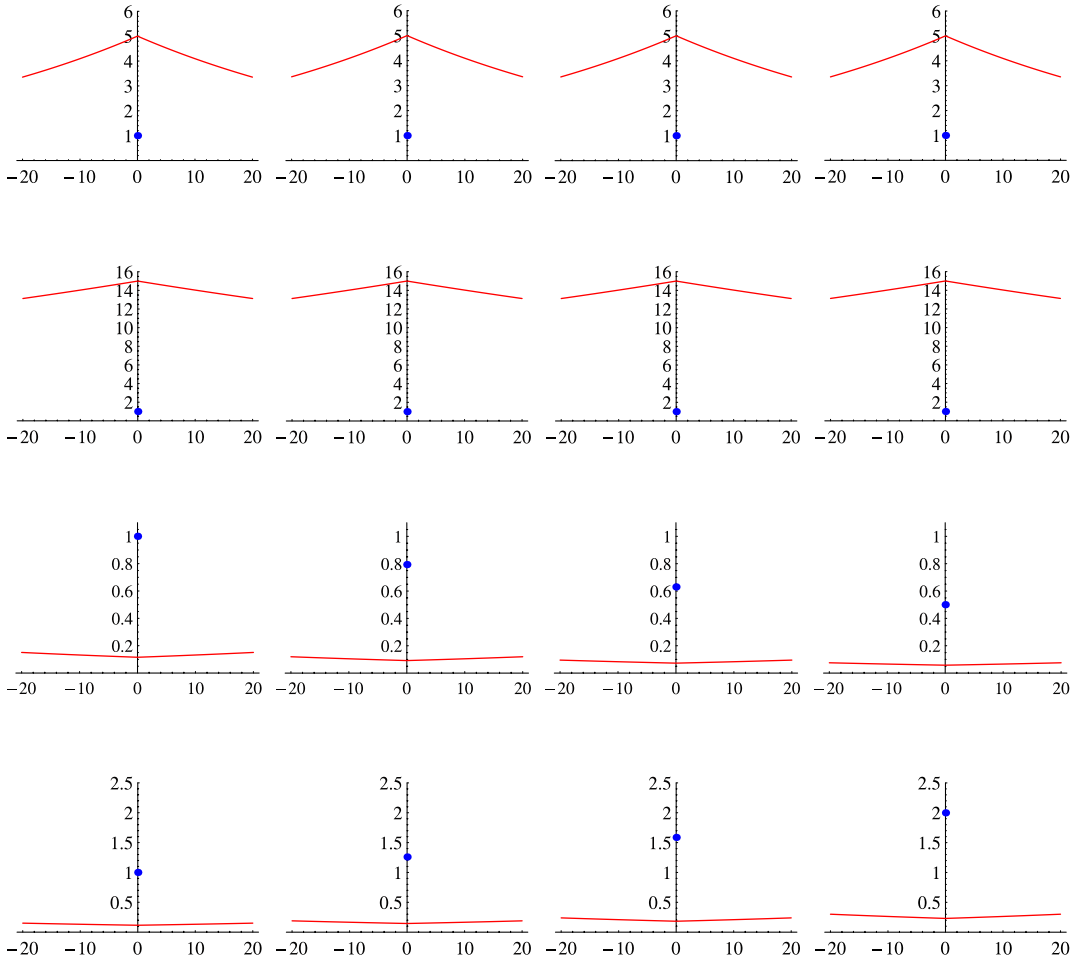

Fig. 12. The time evolution of the eigenfunctions at $t = 0, 20, 40, 60$ for $\tilde{g} = 0.1$ and $\tilde{E}_{\rm d} = -1/2$ in the region $-20 \leq x \leq 20$: from top to bottom, the time evolution of the solid curve (a), the broken curve (b), the dotted curve (c) and the long-short dashed curve (d) in Fig. 9, or the solutions a, b, c and d in Fig. 10, respectively; from left to right $t = 0, 20, 40, 60$. The solutions a and b (the first and second rows) are bound states, and hence there is no time evolution. The solutions c and d (the third and fourth rows) are resonant states. In each panel, the dot indicates $\Psi_{{\rm res},n}(d,t)$ and the curve indicates $|\Psi_{{\rm res},n}(x,t)|$.

Acknowledgements

The authors thank Prof. Satoshi Tanaka for useful discussions. One of the authors (N.H.) expresses his sincere gratitude to Prof. Kiyoshi Kato for helpful comments and continual encouragement and Dr. Myo for helpful discussions at an early stage of the present study as well as useful comments on the final draft. N.H. also thanks Prof. Takeo Kato for useful discussions. This work is supported partly by the Murata Science Foundation and by the National Institutes of Natural Sciences undertaking Forming Bases for Interdisciplinary and International Research

through Cooperation Across Fields of Study and Collaborative Research Program (No. NIFS06KDBT005). One of the authors (N.H.) acknowledges support from a Grant-in-Aid for Scientific Research (No. 17340115) from the Ministry of Education, Culture, Sports, Science and Technology as well as support by Core Research for Evolutional Science and Technology (CREST) of Japan Science and Technology Agency, by the Sumitomo Foundation and by the Casio Science Promotion Foundation. The computation in this work was carried out partly on facilities at the Supercomputer Center, Institute for Solid State Physics, University of Tokyo. One of the authors (T.P.) is grateful to the Foundation for the Promotion of Industrial Science for its support during his stay at the Institute of Industrial Science, University of Tokyo.

Appendix A

—— Expressions in the Three-Dimensional Case ——

In the main text, we focused on the one-dimensional case, expressed by Eq. (2·1). In the present appendix, we give the corresponding expressions in the three-dimensional case, $\hat{\mathcal{H}} = \hat{\mathcal{K}} + \hat{\mathcal{V}}$, where

$$\hat{\mathcal{K}} \equiv \frac{\vec{p}^2}{2m} = -\frac{\hbar^2}{2m}\vec{\nabla}^2 \quad \text{and} \quad \hat{\mathcal{V}} \equiv V(\vec{x}). \tag{A·1}$$

A.1. *The imaginary part of the resonant eigenvalue*

Instead of Eq. (2·5), we define the Hamiltonian expectation value as

$$\langle\psi|\hat{\mathcal{H}}|\psi\rangle_\Omega \equiv \iiint_\Omega \psi(\vec{x})^* \hat{\mathcal{H}}\psi(\vec{x})dV, \tag{A·2}$$

where we consider an integration volume Ω that includes the support of the potential support, $\Omega_{\rm pot}$. The transformation in Eq. (2·9) then corresponds to Gauss's theorem:

$$\begin{aligned}\langle\psi|\hat{\mathcal{K}}|\psi\rangle_\Omega &= -\frac{\hbar^2}{2m}\iiint_\Omega \psi(\vec{x})^*\vec{\nabla}^2\psi(\vec{x})dV \\ &= \frac{\hbar^2}{2m}\iiint_\Omega \vec{\nabla}\psi(\vec{x})^*\cdot\vec{\nabla}\psi(\vec{x})dV - \frac{\hbar^2}{2m}\iint_{\partial\Omega}\psi(\vec{x})^*\vec{\nabla}\psi(\vec{x})\cdot d\vec{S}.\end{aligned} \tag{A·3}$$

In the second term on the last line, the integration is carried out over the surface $\partial\Omega$ of the volume Ω, and $d\vec{S}$ is a vector which is normal to the surface and whose length is equal to the surface element; hence only the normal component of the differentiation $\vec{\nabla}$ contributes to the integral. Subtracting from Eq. (A·3) its complex conjugate, we have

$$2i\,\mathrm{Im}\langle\psi|\hat{\mathcal{H}}|\psi\rangle_\Omega = -\frac{i\hbar}{m}\,\mathrm{Re}\iint_{\partial\Omega}\psi(\vec{x})^*\vec{p}\psi(\vec{x})\cdot d\vec{S}, \tag{A·4}$$

which is followed by the formula (2·12), where we define

$$\langle\psi|\hat{p}_{\rm n}|\psi\rangle_{\partial\Omega} \equiv \iint_{\partial\Omega}\psi(\vec{x})^*\vec{p}\psi(\vec{x})\cdot d\vec{S}. \tag{A·5}$$

The expressions in §2.2 do not differ significantly in the three-dimensional case.

A.2. *The S matrix in three dimensions*

Here we show in three dimensions the equivalence stated in §3.1, that is, the equivalence of seeking the singularities of the S matrix and solving the Schrödinger equation under the boundary condition such that there exists only an outgoing wave.

Let us first review the theory of the S matrix in three dimensions. We show that singularities of the S matrix can give large contributions to the scattering cross section. Consider scattering on the basis of the Schrödinger equation

$$\left(-\frac{\hbar^2}{2m}\vec{\nabla}^2 + V(\vec{x})\right)\psi(\vec{x}) = \frac{\hbar^2 k^2}{2m}\psi(\vec{x}). \tag{A·6}$$

By assuming a solution of the form

$$\psi(\vec{x}) \simeq e^{ikz} + \frac{e^{ikr}}{r} f(\theta; k) \quad \text{as} \quad |\vec{x}| \to \infty, \tag{A·7}$$

we obtain the differential cross section as

$$\frac{d\sigma}{d\Omega} = |f(\theta; k)|^2 . \tag{A·8}$$

Thus, we need to obtain the function $f(\theta; k)$. For this purpose, we expand the wave function (A·7) in partial waves. First, the incident wave is expanded as

$$e^{ikz} = \sum_{l=0}^{\infty} (2l+1) i^l j_l(kr) P_l(\cos\theta) \tag{A·9}$$

$$\simeq \frac{1}{2ikr} \sum_{l=0}^{\infty} (2l+1) \left[e^{ikr} - (-1)^l e^{-ikr}\right] P_l(\cos\theta) \quad \text{as} \quad r \to \infty, \tag{A·10}$$

where j_l denotes a spherical Bessel function and P_l is a Legendre polynomial. We have used an asymptotic form of the spherical Bessel functions in moving from Eq. (A·9) to Eq. (A·10). Next, the scattered wave is expanded as

$$\frac{e^{ikr}}{r} f(\theta; k) = -\frac{e^{ikr}}{2ikr} \sum_{l=0}^{\infty} (2l+1) a_l(k) P_l(\cos\theta), \tag{A·11}$$

with some coefficients $\{a_l(k)\}$. Summing up Eqs. (A·10) and (A·11), we have

$$\psi(\vec{x}) \simeq \frac{1}{2ikr} \sum_{l=0}^{\infty} (2l+1) \left[S_l(k) e^{ikr} - (-1)^l e^{-ikr}\right] P_l(\cos\theta) \quad \text{as} \quad r \to \infty, \tag{A·12}$$

where

$$S_l(k) \equiv 1 - a_l(k) \tag{A·13}$$

is called the S matrix. The cross section (A·8) is calculated from the S matrix as

$$\frac{d\sigma}{d\Omega} = \frac{1}{4k^2} \sum_{l=0}^{\infty} (2l+1) \left|1 - S_l(k)\right|^2 . \tag{A·14}$$

The singularities of the S matrix can thus affect the cross section significantly. In the indirect method, a resonance is defined as a singularity of the S matrix.

We next review the method for computing the S matrix. For this purpose, we introduce the Jost solutions and the Jost functions. We show that singularities of the S matrix are caused by the zeros of a Jost function. Consider a solution of the Schrödinger equation with momentum k and angular momentum l:

$$\psi(r,\theta,\phi) = \frac{\chi(r;k)}{r} Y_{lm}(\theta,\phi). \tag{A·15}$$

For simplicity, we drop the subscript l for various quantities hereafter. The equation for $\chi(r;k)$ is given by

$$\frac{d^2}{dr^2}\chi(r;k) - \left[\frac{2m}{\hbar^2}V(r) + \frac{l(l+1)}{r^2}\right]\chi(r;k) = k^2\chi(r;k), \tag{A·16}$$

where we consider only bounded potentials satisfying

$$\lim_{r\to 0} r^2 V(r) = 0 \quad \text{and} \quad \lim_{r\to\infty} rV(r) = 0. \tag{A·17}$$

Near the origin $r \simeq 0$, Eq. (A·16) reduces to

$$\frac{d^2}{dr^2}\chi(r;k) \simeq \frac{l(l+1)}{r^2}\chi(r;k), \tag{A·18}$$

and hence there are two solutions of the forms r^{l+1} and r^{-l}. The physical solution must be regular at the origin. We thus choose the solution that satisfies

$$\chi(r;k) \simeq r^{l+1} \quad \text{as} \quad r \to 0. \tag{A·19}$$

Far away from the origin, by contrast, there are two potential-free solutions of the forms $\exp(\pm ikr)$. Let $f_\pm(r;k)$ denote the solutions that satisfy

$$f_\pm(r;k) \simeq e^{\pm ikr} \quad \text{as} \quad r \to \infty. \tag{A·20}$$

These are called the Jost solutions. The physical solution $\chi(r;k)$ is a superposition of these two Jost solutions:

$$\chi(r;k) = a_+(k) f_+(r;k) + a_-(k) f_-(r;k), \tag{A·21}$$

with some coefficients $a_\pm(k)$. For later convenience, we change the notation as

$$\chi(r;k) = \frac{1}{2ik}\left(f_-(k) f_+(r;k) - f_+(k) f_-(r;k)\right); \tag{A·22}$$

that is,

$$f_\mp(k) = \pm 2ika_\pm(k), \tag{A·23}$$

which are called the Jost functions. Note that near the origin, the Jost solutions (A·20) are superpositions of solutions of the forms r^{l+1} and r^{-l}:

$$f_\pm(r;k) \simeq b_\pm(k) r^{l+1} + c_\pm(k) r^{-l} \quad \text{as} \quad r \to 0 \tag{A·24}$$

with some coefficients $b_\pm(k)$ and $c_\pm(k)$. The superposition (A·22) in the limit $r \to \infty$ behaves as

$$\chi(r;k) \simeq \frac{f_+(k)}{2ik}\left(\frac{f_-(k)}{f_+(k)}e^{ikr} - e^{-ikr}\right) \quad \text{as} \quad r \to \infty. \tag{A·25}$$

Comparing the asymptotic forms (A·25) and (A·12), we find that the S matrix can be calculated from the Jost functions as

$$S_l(k) = (-1)^l \frac{f_-(k)}{f_+(k)}. \tag{A·26}$$

Therefore, large contributions to the cross section come from the zeros of the Jost function $f_+(k)$.

We can show that the Jost functions, or the superposition coefficients $f_\pm(k)$ in Eq. (A·22), are obtained from the intercepts of the Jost solutions at $r = 0$ as

$$f_\pm(k) = (2l+1)c_\pm(k) = (2l+1)\lim_{r\to 0} r^l f_\pm(r;k). \tag{A·27}$$

For the present purpose, however, we simply set $f_+(k) = 0$ in Eq. (A·22), which reduces to

$$\chi(r;k) \simeq \frac{1}{2ik} f_-(k) f_+(r;k) \propto e^{ikr}. \tag{A·28}$$

This means that we should seek a particular form of the solution $\chi(r;k)$ under the two boundary conditions (A·19) and (A·28). This amounts to solving the Schrödinger equation under the boundary condition that there exists only an outgoing wave. The only difference is that we normally solve for the wave function $\chi(r;k)$ *outward* (starting from the inner boundary condition (A·19) and ending with the outer boundary condition (A·22)), while we normally obtain the Jost function $f_\pm(r;k)$ *inward* (starting from the outer boundary condition (A·20) and ending with the inner boundary condition (A·24)).

Note that in solving the above problem with the two conditions (A·19) and (A·28), we have two undetermined variables, k and $f_-(k)$. Hence, we obtain solutions for discrete values of k.

References

1) G. Gamow, Z. Phys. A **51** (1928), 204.
2) A. J. F. Siegert, Phys. Rev. **56** (1939), 750.
3) R. E. Peierls, Proc. Roy. Soc. London A **253** (1959), 16.
4) K. J. le Couteur, Proc. Roy. Soc. London A **256** (1960), 115.
5) Ya. B. Zel'dovich, J. Exptl. Theoret. Phys. (U.S.S.R.) **39** (1960), 776 [Sov. Phys. JETP **12** (1961), 542].
6) J. Humblet and L. Rosenfeld, Nucl. Phys. **26** (1961), 529.
7) L. Rosenfeld, Nucl. Phys. **26** (1961), 579.
8) J. Humblet, Nucl. Phys. **31** (1962), 544.
9) J. Humblet, Nucl. Phys. **50** (1964), 1.
10) J. P. Jeukenne, Nucl. Phys. **58** (1964), 1.
11) J. Humblet, Nucl. Phys. **57** (1964), 386.
12) C. Mahaux, Nucl. Phys. **68** (1965), 481.
13) L. Rosenfeld, Nucl. Phys. **70** (1965), 1.
14) J. Aguilar and J. M. Combes, Commun. Math. Phys. **22** (1971), 269.

15) E. Baslev and J. M. Combes, Commun. Math. Phys. **22** (1971), 280.
16) B. Simon, Commun. Math. Phys. **27** (1972), 1.
17) L. D. Landau and E. M. Lifshitz, *Quantum Mechanics (Non-relativistic Theory), 3rd edition* (Pergamon Press, Oxford, 1977), §134.
18) R. G. Newton, *Scattering Theory of Waves and Particles, 2nd edition* (Springer-Verlag, New York, 1982), §12.1.4 and Chap. 19.
19) Ed. E. Brändas and N. Elandar, *Resonances* (Springer-Verlag, Berlin, Heidelberg, 1989).
20) V. I. Kukulin, V. M. Krasnopol'sky and J. Horáček, *Theory of Resonances* (Kluwer Academic Publishers, Dordrecht, 1989).
21) A. Nishino and N. Hatano, J. Phys. Soc. Jpn. **76** (2007), 063002.
22) T. N. Rescigno, M. Baertschy, D. Byrum and C. W. McCurdy, Phys. Rev. A **55** (1997), 4253.
23) K. Katō and K. Ikeda, Butsuri **61** (2006), 814 (in Japanese).
24) K. Kobayashi, H. Aikawa, S. Katsumoto and Y. Iye, Phys. Rev. Lett. **88** (2002), 256806.
25) K. Kobayashi, H. Aikawa, S. Katsumoto and Y. Iye, Phys. Rev. B **68** (2003), 235304.
26) K. Kobayashi, H. Aikawa, A. Sano, S. Katsumoto and Y. Iye, Phys. Rev. B **70** (2004), 035319.
27) M. Sato, H. Aikawa, K. Kobayashi, S. Katsumoto and Y. Iye, Phys. Rev. Lett. **95** (2005), 066801.
28) T. Berggren and P. Olanders, Nucl. Phys. A **473** (1987), 189.
29) N. Moiseyev and U. Peskin, Phys. Rev. A **42** (1990), 255.
30) H. Masui, S. Aoyama, T. Myo and K. Katō, Prog. Theor. Phys. **102** (1999), 1119.
31) M. S. Livshits, J. Exptl. Theoret. Phys. (U.S.S.R.) **31** (1956), 121 [Sov. Phys. JETP **4** (1957), 91].
32) H. Feshbach, Ann. of Phys. **5** (1958), 357.
33) H. Feshbach, Ann. of Phys. **19** (1962), 287.
34) J. Okołowicz, M. Płoszajczak and I. Rotter, Phys. Rep. **374** (2003), 271.
35) S. Datta, *Electronic Transport in Mesoscopic Systems* (Cambridge University Press, Cambridge, 1995), §3.5.
36) S. Albeverio, F. Haake, P. Kurasov, M. Kuś and P. Šeba, J. Math. Phys. **37** (1996), 4888.
37) Y. V. Fyodorov and H.-J. Sommers, J. Math. Phys. **38** (1997), 1918.
38) F.-M. Dittes, Phys. Rep. **339** (2000), 215.
39) K. Pichugin, H. Schanz and P. Šeba, Phys. Rev. E **64** (2001), 056227.
40) A. F. Sadreev and I. Rotter, J. of Phys. A **36** (2003), 11413.
41) K. Sasada and N. Hatano, Physica E **29** (2005), 609.
42) K. Sasada and N. Hatano, J. Phys. Soc. Jpn. **77** (2008), 025003.
43) H. Nakamura, N. Hatano, S. Garmon and T. Petrosky, Phys. Rev. Lett. **99** (2007), 210404.
44) N. Moiseyev, P. R. Certain and F. Weinhold, Mol. Phys. **36** (1978), 1613.
45) N. Moiseyev and J. O. Hirschfelder, J. Chem. Phys. **88** (1988), 1063.
46) A. Csótó, B. Gyarmati, A. T. Kruppa, K. F. Pál and N. Moiseyev, Phys. Rev. A **41** (1990), 3469.
47) N. Moiseyev, Phys. Rep. **302** (1998), 212.
48) Y. K. Ho, Phys. Rep. **99** (1983), 1.
49) M. Homma, T. Myo and K. Katō, Prog. Theor. Phys. **97** (1997), 561.
50) T. Myo and K. Katō, Prog. Theor. Phys. **98** (1997), 1275.
51) T. Myo, A. Ohnishi and K. Katō, Prog. Theor. Phys. **99** (1998), 801.
52) R. Suzuki, T. Myo and K. Katō, Prog. Theor. Phys. **113** (2005), 1273.
53) S. Aoyama, T. Myo, K. Katō and K. Ikeda, Prog. Theor. Phys. **116** (2006), 1.
54) A. N. Kolmogorov, Dokl. Akad. Nauk SSSR **98** (1954), 527 [English translation: Los Alamos Scientific Laboratory Translation No. LA-TR-71-67].
55) R. B. Barrar, Celestial Mech. **2** (1970), 494.
56) A. Bohm, M. Gadella and G. B. Mainland, Am. J. Phys. **57** (1989), 1103.
57) T. Petrosky and I. Prigogine, Physica A **147** (1988), 439.
58) T. Petrosky and I. Prigogine, in *Advances in Chemical Physics, Volume 99*, ed. I. Prigogine and S. Rice (John Wiley and Sons, 1997), p. 1.
59) T. Petrosky and G. Ordonez, Phys. Rev. A **56** (1997), 3507.
60) B. Simon, Phys. Lett. A **71** (1979), 211.
61) C. W. McCurdy, Phys. Rev. A **21** (1980), 464.

62) C. Kittel, *Introduction to Solid State Physics, 6th ed.* (John Wiley & Sons, New York), p. 229.
63) H. O. Ohanian and C. G. Ginsburg, Am. J. Phys. **42** (1974), 310.
64) K. O. Friedrichs, Commun. Pure Appl. Math. **1** (1948), 361.
65) T. Petrosky, I. Prigogine and S. Tasaki, Physica A **173** (1991), 175.
66) G. Ordonez, T. Petrosky and I. Prigogine, Phys. Rev. A **63** (2001), 052106.
67) S. Tanaka, S. Garmon and T. Petrosky, Phys. Rev. B **73** (2006), 115340.
68) N. Hokkyo, Prog. Theor. Phys. **33** (1965), 1116.
69) W. J. Romo, Nucl. Phys. A **116** (1968), 617.
70) T. Berggren, Phys. Lett. B **33** (1970), 547.
71) B. Gyarmati and T. Vertse, Nucl. Phys. A **160** (1971), 523.
72) W. J. Romo, J. Math. Phys. **21** (1980), 311.
73) T. Berggren, Nucl. Phys. A **389** (1982), 261.
74) T. Berggren, Phys. Lett. B **373** (1996), 1.
75) R. de la Madrid, G. García-Calderón and J. G. Muga, Czech. J. Phys. **55** (2005), 1141.